

maintains its distinguishing topographical features. As shown in the Bouguer anomaly map, which will be discussed later, the distribution area of the Hualucupen formation area which, is outside the circular basin, shows a high-gravity anomaly, and that of the Las Mellizas formation, which is inside the circular basin, shows a low-gravity anomaly with the northern part of Lago Agrio being its center. The distribution of the low-gravity anomaly corresponds to the volcanic depression structure, except for the western portion.

Fig. 5-7 shows the geologic profile of the Project Area which was prepared based on the results of the geological survey, the gravity prospecting, the exploratory wells and the thermal gradient holes. From the results of the two-dimensional gravity analysis, the depth from the ground surface to the basement rocks (the Hualucupen formation) is estimated to be about 2,000 m at the north side of Lago Agrio where the depth is the largest. The area around Termas de Copahue where geothermal manifestation is observed forms a horst, and it is thought that the depth from the ground surface to the basement rocks is approximately 1,600 m. A throw of about 290 m between COP-2 located on the horst side and COP-1 located on the graben side, which will be discussed later, is confirmed.

Based on the results of the gravity prospecting, it is thought that the lake sediments in the Las Millizas formation are thickly distributed around the north side of Lago Agrio.

(2) Faults

The main faults which affect the geologic structure in the Project Area are described below.

(a) WNW-ESE Faults

The WNW-ESE faults are represented by the one which formed the Paso Copahue-Lago Agrio Graben^{e1)}. These faults cross the caldera and extend to the Chilean side. The fault bordering the north of the graben is a normal fault which passes Chanco C6, and Las

Mellizas (1) and the north shore of Lago Agrio, and runs vertical or with a steep dip towards the southwest direction. Although a throw of about 200 m is observed from the topography around Paso Copahue, the throw becomes small, drawing to the east side.

In addition to the above, faults which determine the flow route of A° Hualcupen and those running at the top of VN. Copahue have been observed. It is considered that the northern and the southern cliffs of circular landform run in this direction, being affected by these faults.

As the WNW-ESE faults are large in scale, it is thought that these faults and the N-S faults were formed by a regional stress field, and the faulting began before the formation of the circular basin.

(b) NE-SW Faults

A number of NE-SW faults are seen in the geothermal manifestation area around Termas de Copahue. These faults can be clearly traced with aerial photographs. Some faults are in the area extending from the northeast slope of VN. Copahue to the northeast of the geothermal manifestation area (Refer to Fig. 4-8). Although the faults running in parallel to each other around Termas de Copahue resulted in a minor depression, the faults generally have minor throws. These are faults of tensional system and generally have steep dips. The width of the fracture zone along the faults observed, ranges from 4 to 5 m.

The NE-SW faults affect the gully to the northwest of VN. Copahue and the Paso Picun Mahuida valley. Some faults are also seen to the southwest of Lago Agrio.

Based on their distribution, the NE-SW faults are deemed to be local ones, closely related with the activity of VN. Copahue, which is the newest volcano in this area.

(c) NW-SE Faults

The NW-SE faults were observed along A° Blanco, which is located to the northeast of Las Máquinas. The major faults are two reverse faults with a strike of N30° to 40°W, and a dip of 60° to 70°W. The width of the fracture along these two faults is about 10 m respectively.

Since geothermal manifestation and alteration zones are not observed on the east side of these faults, it is considered that these faults act as a impermeable zone which shuts off the hydrothermal flow. In addition to the fact that these faults did not cause displacement in the uppermost layer of the Las Mellizas formation, no clear lineaments were found by aerial photographs. This indicates that major displacement in the reverse faults was completed before the completion of the volcanic activity of the Las Mellizas formation.

The NE-SW faults which cut the Las Mellizas formation resulted from local compression due to the volcanic activity of VN. Copahue, and it resulted in reverse faults to the northeast of Termas de Copahue (Pesce, 1987). These reverse faults which Pesca (1987) mentioned are located far more northeast of the aforementioned reverse faults found through this survey.

It is therefore considered that local compression occurred twice due to volcanic activities of the Las Mellizas formation and the Copahue volcanic rocks.

Based on the results of the gravity prospecting, it is thought that the east side of the horst is bounded by the two reverse faults found in this survey, and these faults show a favorable correspondence of upheaval zone of the deep low resistivity layer detected by electrical prospecting.

The relationship between the geothermal manifestation area and the faults is described below, and it should be noted that the lineament

distribution density, which will be discussed later, is generally high in the following areas:

- 1) Las Máquinas and Chancha C6 are located along the WNW-ESE predominant faults;
- 2) Termas de Copahue, Las Maquinitas, and Anfiteatro are located in the area where the NE-SW parallel fault group develops

The LANDSAT imagery and aerial photograph interpretation, show that faults with the same direction of the WNW-ESE and NE-SW are dominant among all the lineaments observed. The WNW-ESE lineaments are distributed throughout almost the entire area. The distribution density of the lineaments is high along the Paso Copahue-Lago Agrio Graben, and some lineaments are found at the north and south ends of the circular basin. As for the NE-SW lineaments, they are densely located around VN. Copahue, Termas de Copahue, and the north side of Lago Agrio.

(3) Geologic Structural History

In the surveyed area, so-called basement rocks are not distributed, but volcanic products and lake sediments which are considered to be of Pliocene and Holocene ages are distributed. The surveyed area is marked by the volcanic activity in the lava plateau extending over the Argentine-Chilean border. Based on the stratigraphic classification and the geologic structure discussed in the previous sections, the geologic structural history of the Project Area is summarized below (Fig. 5-9).

(a) First Stage (Pliocene)

Volcanic activity in this area began from Pliocene time, as far as known to the present, and the Hualcupen formation is formed in this stage. During the volcanic activity, andesite lava and agglomerate were alternately erupted and a stratovolcano, with

the area around Lag. Las Mellizas being the summit, was formed. The formation thickness is more than 1,800 m on the Chilean side.

- (b) Second Stage (the end of Pliocene to the beginning of Pleistocene)

Volcanic depressions accompanied by acidic pyroclastic flows resulted in the formation of a circular basin. Although detailed data on the pyroclastic flow deposits have not been obtained as yet, they are distributed in the east of the surveyed area and they may accumulate inside the circular basin.

- (c) Third Stage (Early to middle Pleistocene)

After the formation of the circular basin, the Las Mellizas formation consisting of andesite, basaltic andesite, and agglomerate erupted at the west margin of the basin and flowed into the circular basin and towards the Chilean side. Meanwhile, a lake was formed on the east side inside the basin and lake sediments were deposited. It is estimated that the lake sediments have two horizons; the sediments were thin on the west side and thick on the east side at both horizons.

The Las Mellizas formation thickly accumulated in the circular basin. During the activity of the Las Mellizas formation, volcanic activity took place to form VN. Bayo and VN. Trolón to the north of the circular basin. Also, as a result of the magmatic activity of the Las Mellizas formation, a horst began to be formed during this stage.

- (d) Fourth Stage (Middle Pleistocene)

Due to consecutive fissure eruptions along A° Trollope, andesite lava was erupted and overflowed outside the circular basin.

(e) Fifth Stage (Late Pleistocene to Holocene)

VN. Copahue became active and basalt lava and pyroclastic rock were erupted. The volcanic activity of VN. Copahue can be roughly divided into three major stages, the last activity took place after the Ice Age. During the periods of volcanic activity, the horst began to be active again and a number of tension system open cracks were developed. The geothermal activity in the surveyed area are thought to have been caused by the rise of the magma chamber and the development of faults during this period.

4. Geothermal Manifestation

In the Project Area, there are five geothermal manifestation areas, one of them being located on the Chilean side, and the overall area being approximately 1.2 km². The four geothermal manifestation areas located on the Argentine side are Termas de Copahue, Las Máquinas, Las Maquinitas, and Anfiteatro, and all of them are on the horst northeast of VN. Copahue. These geothermal manifestation areas are characterized by horseshoe-shaped depressions and form an acidic alteration zone. Many fractures, mainly those in the directions of NE-SW and WNW-ESE, have developed in these geothermal manifestation areas, suggesting that these areas are closely related to the fractures. In the local depressions, there are many fumaroles and hot springs. Although it was difficult to estimate the overall hydrothermal discharge, it is assumed that the supply of geothermal fluid from underground would not be copious since the main discharges are of vapor type and that there are few with flowing hot water. The single geothermal manifestation area on the Chilean side is located at Chancho C6, which is beyond Paso de Copahue across the national border near Termas de Copahue.

The features of each geothermal manifestation area are described as follows:

(1) Termas de Copahue

Termas de Copahue is the largest geothermal area in the Project Area, and there are medical facilities for balneotherapy (Servicio Médico Termal), including hot water pools and steam baths. Although the overall hydrothermal discharge from Termas de Copahue is unknown, the hot water volume flowing out of the largest pool and used for medical treatment is about 200 to 300 l/min by visual measurement and there are no obvious outflows except a few pools and other hot water flows. The medical treatment pools called "Chanco" and "Sulfurosu" are cloudy due to the colloidal sulfur and gas is springing at some places.

The alteration zone of Termas de Copahue mainly consists of white clay and is distributed from the center through the northeast of the depression and the south wall.

(2) Las Máquinas

Las Máquinas is a large geothermal area, but not as large as the area of Termas de Copahue; there are fumaroles surrounding the large hot water pond. The temperature of the pond is not so high and gas is springing at some places. The pond is cloudy due to the colloidal sulfur. The rocks around the fumaroles have been severely altered, some sublimation and mud pots are seen.

In Las Máquinas, two reverse faults were observed downstream of A° Blanco and no alteration is observed on the east side of the reverse faults. The fumaroles in Las Máquinas depression area arrange in the direction of WNW-ESE.

Sanatoriums operated by the Clínica Militar are located in Las Máquinas and used by the public.

(3) Las Maquinitas

Las Maquinitas is the smallest geothermal manifestation area in the Project Area. It consists of the upper and lower small depressions

along the NE-SW faults. At present, the lower depression is active. The temperature of the fluid discharged in these geothermal manifestation areas does not generally exceed 93°C, which is the boiling temperature at this height above sea level, but superheated vapor with a temperature of 132°C has been observed in this area (LATINOCONSULT/ELC-Electroconsult, 1980). Small pools are also found. The flow rate of hot water is only about 50 liters/min together with water from melting.

(4) Anfiteatro

Anfiteatro is located at the far west of the horst. This geothermal manifestation area is not so active but some mud pots and fumaroles are observed. This depression has the form like an explosion crater.

(5) Chancho C6

Chancho C6 is a slender area which extends along the WNW-ESE fault and differs from those developed in the depressions of the geothermal manifestation areas on the Argentine side. Most of the geothermal activity at Chancho-C6 is represented by fumaroles, and traces which indicate only a small discharge of hot water are observed.

In addition to the geothermal manifestation areas mentioned above, there is a water acidified due to gas blowing into the crater lake of VN. Copahue. The lake, which is cloudy, is of a strong acidic type, and emits an irritating smell which might be HCl. Moving downstream on the Rio Agrio, which runs down from this crater lake, a strong acidity of pH 1.2 is observed and the river contains considerable amounts of Cl^- and SO_4^{2-} .

5.1.3 Geophysical Prospecting

1. Gravity Survey

(1) Outline of Prospecting

Gravity prospecting was conducted in 1975 by YPF within the ring-shaped basin. The prospecting area covered was $14 \text{ km} \times 13 \text{ km} = 180 \text{ km}^2$ and the number of measurement points was 285. A Worden gravimeter was used. Three kinds of maps were obtained, these were the maps of Bouguer anomaly of correction coefficients $K = 0.152$, mgal/m ($\rho = 2.23 \text{ g/cm}^3$), and $K = 0.200$ mgal/m ($\rho = 2.59 \text{ g/cm}^3$), and the map of residual gravity ($R = 1.5 \text{ km}$) of $K = 0.215$ mgal/m.

(2) Overall Structure

Fig. 5-10 ⁽²⁶⁾ shows the map of Bouguer anomaly of correction coefficient $K = 0.215$ mgal/m.

- (a) According to the figure, expansion of high gravity zone can be seen from Termas de Copahue to Las Máquinas, but except for that, the overall structure is in a neat ring shape, which reflects a volcanic structural depression.
- (b) Two dimensional two layer analysis on a-a' line and b-b' line made by JICA team are shown in Fig. 5-10. For a-a' line the Hualcupén Formation, that is exposed on the caldera wall near both ends of the line, was used as control point. The analysis was performed on the cases of $\Delta\rho = 0.20, 0.25, 0.30 \text{ g/cm}^3$, respectively. For b-b' line, analysis was performed using the Hualcupén formation, that is exposed on the caldera wall near the eastern end, and the results of the analysis of a-a' line at the point of intersection therewith, as control data. The results are shown in Fig. 5-11.
- (c) The depth profile is considered to reflect practically the entire top of the Hualcupén formation that constitutes the base of the

basin. Especially, it is considered that the depth profile at $\Delta\rho = 0.25 \text{ g/cm}^3$ reflects the basin structure relatively well. On the east of the b-b' line and on both sides of the a-a' line, the depth of the Hualcupén formation may possibly be shallower than that of at $\Delta\rho = 0.25 \text{ g/cm}^3$, closing to the analyzed depth at $\Delta\rho = 0.3 \text{ g/cm}^3$.

(3) Local Structure

- (a) Expansion of a high gravity zone exists from Termas de Copahue to Las Máquinas. A high gravity spine of about 2 to 3 mgal stretches east-southeast from there having width of about 4 km along the b-b' line a-a' center. A horst structure may exist in this high gravity zone. However, as the direction of the high gravity zone matches the flow of the lava unit of the Las Mellizas formation, it may have been affected significantly by the thickness of high density lava.
- (b) Northwest trending reverse faults that dip southwest were confirmed near Las Máquinas. The isogravity contour shows a linear steep slope along these reverse faults exhibiting a high gravity on the west side thereof. This may be due to the horst structure formed by these reverse faults.
- (c) A low gravity zone stretches from Lag. Las Mellizas (1) to Caviahue in the direction of WNW-ESE. The fault is estimated with several findings along the northeast edge of this low gravity zone. Therefore, it may be possible that this low gravity zone shows a graben accompanying the fault.

2. Electrical Prospecting

(1) Outline of Prospecting

Electrical prospecting (Schlumberger method) was performed in two periods, first in 1980 and then in 1982 by LATINOCONSULT/ELC-Electroconsult.

The first prospecting^{c1)} was performed in a wide area from near Termas de Copahue to near Caviahue, covering 56 measurement points with the maximum electrode spacing of $AB/2 = 2,000$ m (partly 700, 1,000, 3,000 m). As 13 points of these 56 measurement points were taken on the orthogonal lines in two directions, the total number of data measured was 69.

The results were summarized in 4 maps of apparent resistivity, 13 profiles of resistivity layers, and a map of the top of the high resistivity layer, etc.

The second prospecting^{c3)}, a deep electrical prospecting, with the maximum electrode spacing of $AB/2 = 5,000$ m, was performed to confirm the existence of the deep low resistivity layer on which an indication was obtained in the first prospecting. Of these 7 measurement points, as 3 measured points were taken on lines in 3 to 4 directions in order to check the anisotropy, the total number of data measured was 15. The results were summarized by adding the results of further analysis of the first prospecting data in 6 profiles of resistivity layers, a map of the top of the high resistivity layer, and a map of the top of the deep low resistivity layer, etc.

In addition to these, in 1987, another prospecting was carried out by CREGEN at the section northeast of Lago Agrio with 11 measurement points ($AB/2 = 1,500$ m).

(2) Resistivity Layer and Its Resolution

There may be factors that partly accompany the subjective decision in the analysis of the VES curve, but the results of a close examination of distribution of apparent resistivity and the electrical logging at well COP-1 and 2 show that the analysis of the first prospecting is generally appropriate. However, for the deep low resistivity layer, the results of the analysis of the second prospecting were applied.

(a) Fig. 5-12 shows the outline of the distribution of the analyzed resistivity layers. The resistivity layers in the prospecting area were analyzed into 3 or 4 layers inside of the triangular area in Fig. 4-16 (hereinafter to be referred to as "triangle zone"), and into 2 or 3 layers outside of the area. These resistivity layers can be classified into the following six units:

- ① Surface high resistivity layer : ±170 ohm-m
(100 to 700 ohm-m)
- ② Peripheral medium resistivity layer : ±20 ohm-m
(11 to 30 ohm-m)
- ③ Shallow low resistivity layer : ±8 ohm-m
(4 to 14 ohm-m)
- ④ Intermediate depth high resistivity layer : ±150 ohm-m
(70 to 38 ohm-m)
- ⑤ Deep low resistivity layer : ±7 ohm-m
- ⑥ Deep high resistivity layer : ±150 ohm-m

However, the resistivity values on the vicinity of the manifestations were low at each layer, analyzed as follows:

①' : ±20 ohm-m

③' : ±5 ohm-m

④' : ±45 ohm-m

In addition to these units, a thin high resistivity layer distributes near the ground surface (40 m or shallower). In the profiles this layer was included in ① layer.

- (b) As can be seen from Fig. 5-12, the most characteristic features are that a distinctive difference can be recognized between the inside and outside of the above mentioned triangle zone and the inside of the triangle zone is characterized as the upheaval zone of so-called high resistivity basement ④. In other words, the resistivity structure up to near the depth of 1,000 m can be analyzed in two layers outside the triangle zone, i.e. high resistivity layer ① and medium resistivity layer ②. On the other hand, it can be analyzed in 3 layers inside the triangle zone, i.e. high resistivity layer ①, low resistivity layer ③ and high resistivity layer ④.

These characteristic differences are clear from the type of the VES curve. From the following VES curve, the reflection of high resistivity layer was clearly seen in the VES curve inside the triangle zone, but there was no such sign outside.

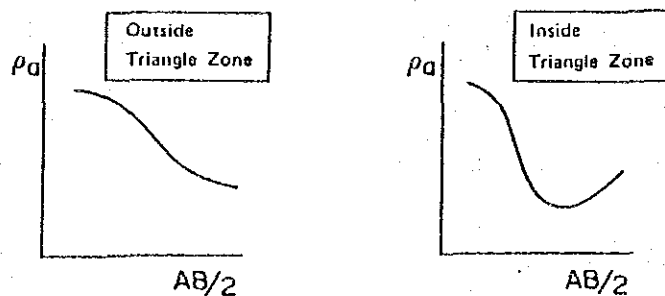


Fig. 5-13 Characteristics of VES Curves

(c) Deep low (or high) resistivity layers were detected at the depth of 800 to 1,800 m. In general, the limit depth of the lowest layer which can be detected is about 1,000 m at $AB/2 = 2,000$ m and about 2,000 to 2,500 m at $AB/2 = 5,000$ m. Therefore, the depth and resistivity values of deep low (or high) resistivity layers are qualitative for each layer and the errors are large.

(d) The existence of the deep low resistivity layer is important data for discussing the geothermal model. In the prospecting performed this time, the deep low resistivity layer was detected at nine measurement points (9/10, 31/32, 7/8, 5/6, 22/23, D-I, II, III, 13) and the configuration thereof can be divided into two types, one that is distributed horizontally near the depth of 1,800 m $\textcircled{0}$ and an other that is detected at a relatively shallower depth near Termas de Copahue and Las Máquinas $\textcircled{0}'$ (Fig. 5-12). Although the existence of the deep horizontal low resistivity layer $\textcircled{0}$ was not confirmed with high accuracy, this layer is considered to be correlated with a chloritized alteration zone that is widely distributed inside the triangle zone in constructing a model of the geothermal system.

(3) Interpretation of Each Resistivity Layer and its Distribution

On the basis of the resistivity structure mentioned in the previous section, the interpretation of each resistivity layer and its distribution are described below:

(a) Surface high resistivity layer ($\textcircled{0}$ ± 170 ohm-m, $\textcircled{0}'$ ± 20 ohm-m)

- 1) This layer is distributed throughout the entire area prospected. Its depth is 100 to 150 m inside the triangle zone and 150 to 300 m outside the triangle zone. It appears that there is a strong possibility that the bottom of this layer reflects the groundwater level.

- 2) On the vicinity of the manifestations the layer becomes thinner, i.e. about 50 m in thickness, and its resistivity value also decreases.

(b) Peripheral medium resistivity layer (Q ± 20 ohm-m)

- 1) This layer is distributed thick below the depth of 150 to 300 m outside the triangle zone, showing a relatively uniform resistivity value, i.e. 11 to 30 ohm-m.
- 2) Assuming that the resistivity value of the lava layer to be 300 ohm-m, the proportion of argillaceous rocks would be about 25%.

The resistivity value of this layer to the southeast of the prospecting area near Lago Agrio shows a somewhat lower value, i.e. 11 to 15 ohm-m. This probably means that the content of argillaceous rocks is higher to the southeast compared with that to the northwest of the prospecting area.

(c) Shallow low resistivity layer (Q ± 8 ohm-m, Q' ± 5 ohm-m)

- 1) The depth of the top of this layer shows 100 to 150 m, tending to be shallower around the manifestations on the north and east sides of the triangle zone, and gradually becoming deeper on the southwest side away from the manifestations. The trend is similar in the case of layer thickness, i.e. the thickness shows 300 to 600 m, also becoming thicker toward the southwest.
- 2) In the vicinity of the manifestations, the layer is distributed from near the depth of 50 m to near the depth of 200 m, with the top depth and layer thickness being considerably shallow and thin, the resistivity value is also somewhat lower, i.e. ± 5 ohm-m. As local anomalies in the shallow low resistivity layer have not been recognized

except these vicinities, it is considered that the outflow of geothermal fluids to the ground surface has been limited only to these present fumarole zones.

- (d) Intermediate depth high resistivity layer (\approx ± 150 ohm-m, \approx 45 ohm-m)

Fig. 4-14 shows a map of the top of the high resistivity layer. Depth from the ground surface to the top of this layer is generally 400 to 800 m, being shallower on the fumarole zones and deeper on the southwest side. In the vicinity of the manifestations the depth becomes extremely shallow, i.e. 100 to 200 m showing that the vapor dominated zone draws near the ground surface. The resistivity value in the vicinity of the fumarole zone is low, i.e. 45 ohm-m.

- (e) Deep low resistivity layer (\approx ± 7 ohm-m)

Fig. 5-15 shows the detected depth of the deep low resistivity layer. Of these, the deep low resistivity layer that is indicated as a horizontal layer near the depth of 1,800 m might be considered for the time being to correspond to argillaceous basements which LATINOCONSULT/ELC-Electroconsult (1982) suggested. Considering, however, that this layer is viewed as a high resistivity layer outside the triangle zone, the possibility is extremely small. From the viewpoint of reservoir structure, it is reasonable to consider this layer as corresponding to the hot water zone with a high concentration of salinity.

- (f) Deep high resistivity layer (\approx ± 150 ohm-m)

This layer was detected near the depth of 1,500 m in the following measurement points. Those were 59, 56, 63, 60 on the north side of the triangle zone and 42, 3, 16, 29, 28 on the north side of Lago Agrio. In addition the same symptoms were recognized at 13, 17, 45 and 30.

Therefore, despite the considerable errors due to the large depth, there is a strong possibility that the layer is distributed throughout the prospected area except for the triangle zone. In this case, there is a strong possibility that this layer corresponds to the Hualcupen Formation. Inside the triangle zone this layer is viewed as a low resistivity layer. This low resistivity layer is considered a local phenomenon originating from the brine.

(g) Peripheral boundary of upheaval zone of high resistivity basement found by the electrical prospecting practically matches the following faults:

- 1) Boundary on the southwest side: the fault from Chanco Có through Lag. Mellizas (1) and continuing to the north shore of Lago Agrio.
- 2) Boundary on the north side: the fault that extends in the WSW-ENE direction passing about 1.5 km north of Termas de Copahue.
- 3) Boundary of the east side: two parallel reverse faults that extend in the NW-SE direction passing about 1 km northeast of Las Máquinas.

(h) Low resistivity zone in the northeast of the triangle zone

As shown in Figs. 5-12 and 5-15, a swelling of the deep low resistivity layer was detected in the vicinity from Termas de Copahue to Las Máquinas. The resistivity layers above this swelling zone show a low resistivity value as compared with others, i.e. ④', ③', ①' respectively, forming a low resistivity zone as a whole. This low resistivity zone coincides with the reverse faults mentioned above in the deep section. This low resistivity zone is considered to indicate that the periphery of the up flow path of geothermal fluids was widely altered.

5.1.4 Geochemical Survey

1. Chemical Composition of Ground Surface Water and Hot Spring Water

(1) Analysis of previous survey results

The following three surveys were conducted systematically with regard to the chemical analysis:

- (a) There are 16 pieces of data available from Jurio (1979)⁽²⁰⁾.
- (b) LATINOCONSULT/ELC-Electroconsult (1980)⁽¹⁾ performed analysis of major ions at about 40 points with Termas de Copahue as a center. In addition, measurements were taken of pH and electric conductivity only at about 40 points.
- (c) As a part of the report on isotopes compiled by Panarella et al. (1985)⁽¹⁸⁾, in which chemical analysis values of water were reported for 9 points.

Analysis was made on 40 points in (b), less 3 points in the Copahue area where precise locations are unknown, plus 3 points in (c) that are located in the area.

Because the location of points in (a) above is unclear, the data is too old, and the effective digit is rougher by one unit than the others, all data from (a) was disregarded.

Fig 5-16 and Table 5-3 show the location of sampling and results of analysis, and Fig. 5-17 and Fig. 5-18 show the key diagram and the hexadiagram, respectively.

(2) Consideration

There are four geothermal manifestation areas in this region. The corresponding sample numbers of hot spring water are as follows:

- (a) Las Máquinas Nos. 28, 29, 30, 31, 32
- (b) Las Maquinitas Nos. 33, 34
- (c) Anfiteatro Nos. 35, 36, 37
- (d) Termas de Copahue Nos. 38, 39, 40

Of these hot spring water samples except Nos. 30 and 37 (reasons for exception will be explained later), when looking at the relative ratio of quantity of major anions, the hot spring water of Las Maquinitas and Anfiteatro can be classified as SO_4 type and that of Termas de Copahue as HCO_3 type. On the other hand, when looking at major cations, i.e., Na, K, Ca, and Mg, a common tendency can be seen in that the volume of soluble materials of these cations is very small except at Termas de Copahue where the volume was slightly larger compared with the three other areas. In other words, the hot spring water at Termas de Copahue contains more carbonate. With regard to the relative quantity ratio, the hot spring water at Las Máquinas, Las Maquinitas and Anfiteatro scarcely contains Ca. On the other hand, another cation worthy of notice at Las Máquinas, Las Maquinitas and Anfiteatro is NH_4 . The water of these hot springs can be divided into two extremes, i.e. those which contain NH_4 and those which contain no NH_4 . Although it is not considered a good correlation, it appears that the hot spring water with a high pH does not contain NH_4 . It is expected in future to perform analysis for NH_4 in the hot spring water at Termas de Copahue as well as continued analysis of hot spring water at Las Máquinas, Las Maquinitas, and Anfiteatro.

Summarizing the above examination, the hot spring water of Las Máquinas, Las Maquinitas and Anfiteatro may be classified as the $\text{NH}_4\text{-SO}_4$ type and that of Termas de Copahue as the HCO_3 type (cation unknown). Taking into account that a large quantity of volatile components are contained, these hot springs suggest to originate from the blowing of gas and steam-heating from deep underground into groundwater at shallower levels.

As shown in Table 4-3, many samples (Nos. 1 - 27) of river water, lake water, and groundwater in this area have been analyzed. Much of the data shows small quantities of soluble materials and low levels in both electric conductivity and discharge temperature, suggesting that they are ground surface water or shallow groundwater that is similar to meteoric water. Several of the peculiar points are as follows:

- (a) Samples of Nos. 3, 4 and 11 along the Rio Agrio contain many soluble materials, in particular SO_4 and Cl , and have low pH values. Particularly, No. 11 shows the lowest pH and the largest quantity of soluble materials among the analysis values for this area. This is assumed to be due to the existence of the crater lake, Lag. del Volcán, as its origin; the lake water is estimated to contain soluble materials in quantity, such as Cl and SO_4 , thereby affecting the river water downstream, causing a high Cl and SO_4 content and a low pH value. The effects extend as far as No. 5 at Lago Agrio. No. 2, although in a different water system, is also assumed to have been affected by distribution of debris flow attributable to Lag. del Volcán. Although the chemical analysis values of water from this crater lake are not available, because the river water downstream contains an extremely large volume of soluble materials such as Cl and SO_4 and HCl gas hangs in the air near the surface of the lake, the gas that blows into the lake water is considered to be a high temperature volcanic gas consisting mainly of HCl and SO_2 (or H_2S).
- (b) The volume of soluble materials in most of the samples except those of ground surface water suggests that remarkably little ground water is affected by the water of Lago del Volcan. Of these, Nos. 6, 7, 8, 13, 20 and 24 show a slightly large volume of soluble materials. As No. 20 is located near Termas de Copahue and Nos. 6 and 13 is located downstream from the geothermal manifestation area, they are assumed to have been affected by geothermal manifestation. It is possible that the remaining Nos. 7, 8, and 24 show geothermal manifestation though slightly, suggesting that the geothermal manifestation extends

nearly to Lag. Las Mellizas in addition to Las Máquinas, Las Maquinitas, Anfiteatro, and Termas de Capahue.

2. Chemical Composition of Gas

(1) Analysis of Previous Survey Result

The analysis of gas from fumaroles and the exploratory well was performed several times in the past, the summary of which is as follows:

<u>Derivation</u>	<u>Bibliography</u>	<u>Content</u>
1) Jurio (1977)	C20	11 points in total including 2 points at Chancho C6
2) LATINOCONSULT/ ELC-Electroconsult (1980)	C1	Note) 6 points, 12 pieces of data
3) LATINOCONSULT/ ELC-Electroconsult (1981)	C2	3 pieces of data including COP-1
4) COPADE (1982)	C4	13 pieces of data in total including 7 data of COP-1
5) PISA (1986)	C22	10 points in total including 1 point each of COP-1 and COP-2

Note) In addition there are 8 pieces of data available of gas composition except CO₂, which are disregarded.

(2) Consideration

Table 5-4 shows the gas composition in the geothermal fluid from fumaroles and exploratory wells by area. Fig. 5-19 shows the relative ratios of CO₂, H₂S, and R-gas. Also shown are the results of COP-1 and -3 conducted by JICA. From the figure, the following comments can be made:

Most of the gas in this area is remarkably rich in CO₂ (larger than 90%). The only notable exception is the one at Chancho C6, which

contains relatively less CO₂ compared with others. H₂S and H₂ account for about 10 - 16%, respectively.

The gas of Las Máquinas, Las Maquinitas, Anfiteatro, Termas de Capahue, and COP-1 and -2 shows the CO₂ content is larger than 90% and the H₂S content is smaller than 1%. This composition is rather closer to that of gas accompanied by hot spring rather than that of common volcanic gas or fumarolic gas.

The gas composition of Las Máquinas and that of COP-1 are extremely similar, and cannot practically be distinguished from the viewpoint of gas composition. This may arise because both locations are topographically close and the vapor from the same reservoir as COP-1 penetrates, rises through fractures and reaches the ground surface of Las Máquinas directly.

It should be noted that the COP-3 gas analyzed in this project contained 95% CO₂, very close to the composition of Las Maquinitas gas.

Table 5-4 also shows the temperature calculated from the gas composition (D'Amore and Panichi, 1980). The results of all samples except 4 samples fall in the range between 205 and 230°C. Also, there are not remarkable differences between areas, all showing extremely close temperatures to those confirmed at COP-1, -2 and -3.

3. Isotopic Composition of Meteoric Water and Geothermal Fluid

(1) Analysis of Previous Survey Result

As shown in Table 5-5, the isotopic composition of the Project Area from Panarello et al. (1985)⁽¹⁸⁾ is available. According to the reports, sampling and quantitative analysis were done on 19 points between February and April 1985. Also, the reports quoted data from 1982 for COP-1. Subsequently, an isotope analysis of geothermal fluid from COP-1 and -2 were done by IIRG (Italy) in November 1986. The sampling locations and relation between $\delta^{18}\text{O}$ and δD are shown in Figs. 5-16 and

5-20, respectively. The results of the present JICA survey are also shown here.

(2) Consideration

As shown in Fig. 5-20, most data points with the exception of Las Máquinas, Las Maquinitas, COP-1, -2 and -3 occupy positions close to the global meteoric water line, the equation being $\delta D = 8 \times \delta^{18}O + 10$ (Creig, 1961), suggesting that hot spring water, ground surface water, and groundwater in this area are basically of meteoric water origin.

The hot spring water and ground surface water (I-9-13,15) in the vicinity of Termas de Copahue have similar values, i.e. $\delta D = -11 \sim -12\%$ and $\delta^{18}O = -82 \sim -85\%$. These values apparently differ from those of meteoric water near the altitudes of 2,200 - 2,300 m mentioned above. In other words, the origin of the hot spring water of Termas de Copahue is considered to be meteoric water, which did not fall in the area of higher altitude but fell relatively near there and permeated into the ground.

The isotopic composition of the fumarolic vapor (I-6, 7) of Las Máquinas and Las Maquinitas is close to that of the vapor (I-1, 4) from COP-1 and -2 at the early stage of production test to be mentioned later, suggesting that they have the same origin.

The history of isotopic composition of condensed water from COP-1 and -2 shows an increase in both δD and $\delta^{18}O$. This may be due to changes in vapor saturation at deeper levels rather than changes in the isotopic composition of the original geothermal fluid that is the source of the vapor, and the possibility that the quantity of the geothermal fluid stored in the reservoir is smaller compared with the production rate was pointed out by D'Amore et al. (1987).

With regard to 3H , ground surface water and groundwater in the shallow section (I-14 - 22) have a similar value of about 2 - 5 TU. Taking into account that no larger values were obtained, these values are considered to show 3H content in the meteoric water at present or in the

recent past in this area. The ^3H content of the hot spring water at Termas de Copahue is of similar value as mentioned above, but is slightly lower, i.e. about 2 - 3 TU. Therefore, the origin of this hot spring water is considered to be meteoric water that fell in the recent past. Although changes in ^3H content of the meteoric water in this area after 1950 are unknown, assuming a value of 4.8 TU, the maximum value among the samples for meteoric water, and assuming the value of hot spring water at Termas de Copahue as 2.5 TU, the average value of 3 samples, and finally assuming that it is a closed system, the meteoric water is estimated to be rainfall that is 10 years old.

The ^3H content of the vapor of Las Máquinas and Las Maquinitas and the vapor from COP-1 and -2 all show low values, i.e. below 1 TU. It is not clear whether this shows an old origin of rainfall or a result of the fractional effect of isotopes at the time of the gas-liquid separation (probably the effect of the latter would be stronger).

4. Soil Geochemical Survey

In the soil geochemical survey, three items were measured: ground temperature at a depth of 1 m, CO_2 concentration in soil gas, and Hg concentration in soil (Pedro et al. 1986).

The measurements were taken covering 70 points in the Copahue area and 50 points in the Cavihue area, the measurement points being laid out in a grid pattern with a spacing of 500 m. Measurement was implemented between January 1986 and February 1986 and for the ground temperature at a depth of 1 m, day history measurement and altitude correction were performed.

According to the results of measurement, no remarkable anomalies are recognized in the Cavihue area. On the other hand, in the Copahue area, remarkable anomalies are recognized in temperature, CO_2 concentration, and Hg concentration.

Fig. 5-21 shows the results of the survey in the Copahue area. In the geothermal manifestation areas of Termas de Copahue and Las Máquinas, all

three items of measurement were higher, i.e. ground temperature at a depth of 1 m (residual temperature > 4.5°C), Hg concentration (>100 ppb), and CO₂ concentration (>0.15%), suggesting that these areas have been geothermically active. In the periphery of Las Maquinitas, each measured value shows a relatively high value.

On the other hand, on the northeast of the Project Area, there is an area where Hg and CO₂ concentration are higher, i.e. > 20 ppb for Hg and > 0.1% for CO₂. The area is covered with sediments carried by small rivers that flow downstream from Las Maquinitas and Las Máquinas and is thickly covered with vegetation. Therefore, it is possible that Hg concentration reflects the effect of sediments and the CO₂ concentration the effect of vegetation. Similarly, as the high CO₂ concentration area on the southeast of Co. de Las Máquinas (>0.15%) shows a low value for both ground temperature at a depth of 1 m and Hg concentration, the high CO₂ concentration may be considered due to the effect of vegetation.

5. Geochemical Survey on Wells

(1) Scope of Survey

JICA conducted the geochemical survey on COP-1 and -3 during the COP-3's production test, under cooperation of CREGEN, as summarized in Table 5-6.

Among the above items, only the gas vapor ratio was measured during the field survey, and other items were analyzed in Japan with pre-treatment being done on site.

In addition, the same survey was conducted by CREGEN.

(2) Survey results

The results of chemical analysis of geothermal fluid from COP-1 and -3 during the period of production test on COP-3 are presented in Tables 5-7, 5-8, and 5-9.

(a) Gas vapor ratio

As gas accounted for a large portion in gas vapor ratio, 10 measurements were made in COP-3 to obtain the mean value.

① COP-1

Gas content in gas vapor ratio was 5.8%. (Note: indicated in volume Z, applied to the rest of the section, unless otherwise specified)

② COP-3

Gas content was 5%, similar to 3.5% - 5% measured in the initial production phase of COP-2. This data agrees with that observed in the CREGEN survey. (62.8 lN Gas/kg Vapor = 5%, 2/June/1991)

(b) Gas composition

① COP-1

Gas unabsorbed in an alkaline solution, R gas, was 8.75%. Composition is shown in Table 4-7.

② COP-3

95.79% of gas was CO₂, and H₂S accounted for 0.39%. (as measured by wet chemical analysis in which H₂S was absorbed in NaOH solution and fixed by cadmium acetate) On the other hand, H₂S concentration measured by CREGEN on site was 0.45%. (with Kitagawa gas detection tube)

Percentage of R gas was 3.82%.

(c) Condensate

① COP-1

pH was 5.6 and electric conductivity was 470 $\mu\text{s}/\text{cm}$. The concentrations of major species were low and TSM was 24 mg/ℓ . The concentration of HCO_3^- was relatively high, reflecting the major content of CO_2 in the gas.

② COP-3

pH was 5.8 and electric conductivity was 830 $\mu\text{s}/\text{cm}$. The concentrations of major species were low and TSM was 17 mg/ℓ . Compared to COP-1, boron (B) and ammonia (NH_4^+) compositions were higher, while other species were in similar order.

(d) Hot water content

① COP-1

COP-1 produces steam only, not accompanying hot water.

② COP-3

During the COP-3 production test, a small amount of hot water (0 - 0.8 /h) came out at the triangular weir box. However, the results of analysis, shown in Table 5-8, do not suggest the production of deep brine, because of the electric conductivity of 300 $\mu\text{s}/\text{cm}$, Cl⁻-concentration of 2.2 mg/ℓ , and very small concentrations of major species.

Thus, hot water produced from COP-3 is not the original brine but the condensate.

(e) Isotope

① COP-1

Deuterium and Oxygen 18 of COP-1 measured in this survey, shown in Table 5-9 and Fig. 5-20, are different from previous data; the former was -11.5% and the latter -100.1%, 15-25% and 3-4% lighter respectively.

There are two possible causes for this: if the condensate is mixed in the steam, δD and $\delta^{18}O$ could be reduced by a few tens % and a few % respectively due to isotopic fractionation occurring in flushing through the pipeline; or if these are original isotopic values, recharge conditions or feed points may have changed. Considering that samples are taken from a branch pipe 5 m down from the main steam line, the possibility of the isotopic fractionation is high.

On the other hand, $^{13}C/^{12}C$ was - 8.9%, compared to -10.9% measured in COP-1 in 1985, with the same order (Sierra et al. 1990)^{c38}.

$^{34}S/^{32}S$ was +3.6%.

② COP-3

δD and $\delta^{18}O$ values of condensate (I-24) from COP-3 were -85.3% and -9.4% respectively, approximately the same as those measured in COP-1 and COP-2. On the other hand, δD and $\delta^{18}O$ of hot water (I-25) obtained from the triangular weir box of COP-3 were -62.4% and -4.3% respectively, which agree with isotope fractionation at 100 - 114°C, indicating that the hot water was produced by dynamic process in the separator. From these two values as well as the steam and water flow rates, the isotope ratio in original steam was calculated at -84% for δD and -9% for $\delta^{18}O$.

As shown in Fig. 5-20, I-24 is plotted on the line connecting I-4 and I-5 of COP-2.

$^{13}\text{C}/^{12}\text{C}$ was -9.3‰ for the condensate, which was approximately the same in COP-1, and -14.1‰ for the hot water.

$^{34}\text{S}/^{32}\text{S}$ was -3.6‰ for the condensate and +12.3‰ for the hot water. However, the difference between these values does not seem to be intrinsic, rather it is a result of heavy ^{34}S concentrating in the hot water while passing through the separator, and others.

^3H concentration was less than 0.3TU, and that in the steam from COP-1 and -2 was less than 1TU. (Sierra et al, 1990)^{c38)}

These values may be affected by isotopic fractionation during the steam-water separation process.

(3) Consideration

COP-3 produced 9.4 ton/hour of steam at wellhead pressure of 1.4 kg/cm². Although hot water flew out at the triangular weir box at 0 - 0.9 ton/hour during the production test, comparison of chemical compositions of the hot water and steam revealed that the hot water was the condensate with the changed properties, not brine in the reservoir.

Gas content in the gas vapor ratio was relatively high at 5%, 95% of which was CO₂. In addition, the presence of NH₄ gas is suspected from NH₄⁺ (21 mg/l) in the condensate, although no analysis was conducted in this survey.

Although ^3H value was less than 0.3TU, its age is not known because of the possible influence of isotopic fractionation.

Several attempts have been made to determine temperature (T) and molar steam fraction (y) of reservoir from gas composition in the vapor-dominated field, by D'Amore and Celati (1983), and D'Amore and Truesdell (1985) etc. D'Amore and Truesdell (1985) points out the need for verification of this geochemical thermometer in a number of geothermal fields.

An attempt has been made by CREGEN (Sierra et al. 1990)^{c38} to estimate the condition of the reservoir in the vapor dominated system of COP-1 and -2 by using this gas-geothermometer.

By using the equation D'Amore and Truesdell (1985) and gas composition data analyzed during the COP-3 production test, temperature is estimated at 200°C and the molar steam fraction (y) is slightly over 1. On the other hand, the temperature of 215°C was calculated by the gas geochemical thermometer of D'Amore and Panichi (1980), as shown in Table 5-4.

Considering possible errors in these values, T=200-215°C and y=1 seem to be appropriate.

In this calculation (for equations of D'Amore and Truesdell (1985)), the molar distribution coefficient between steam and liquid phases for the gas species was taken from that of Giggenbach (1981).

These values (T=200-215°C, y=1) are very similar to those calculated for COP-1 and -2 in their earlier production phase; for COP-1, T=175°C and y=1 at the initial phase (1982), which were changed to T=245-250°C, y=0.45 in 1987. This initial condition appears to be 'gas cap' reported in the Geysers, which lasts for about one month during the initial production phase. (Sierra et al. 1990)^{c38}

Similarly, COP-2, T=200°C and y=1 at the initial phase (1986) were changed to T=235°C and y=0.35 in 1987.

The changes in T and y with production at COP-1 and -2 suggest the possibility of similar changes in COP-3.

Thus, the monitoring of gas vapor ratio and gas compositions of the geothermal fluid of COP-3 is recommended to check their changes with time.

6. Conclusion of Geochemical Survey

From the foregoing, as the origin of hot springs and fumaroles in this area, the following model is considered:

A vapor system of about 230 - 240°C exists deep below the ground and the geothermal fluid in the reservoir is considered to consist of vapor. As the fumarolic gas of the four geothermal manifestation areas has a resemblance in composition, the geothermal fluid in the reservoir should also show a homogeneous composition. In other words, non-condensed gas in the reservoir consists mostly of CO₂. A part of it rises through fractures, etc. and forms a fumarole as it reaches the ground surface. On the other hand, as the gas blows into the groundwater of meteoric water origin at a shallow level below ground and heats it, an HCO₃ type hot spring is formed at Termas de Copahue.

However, SO₄ type hot spring water exists at Las Máquinas, Las Maquinitas and Anfiteatro. As SO₄ type water in many cases indicates a low pH, it is considered a possibility that SO₄ type water is formed because carbonic acid escapes into the air as CO₂. However, as the amount of H₂S in the gas is too small against SO₄ in the hot spring water, it is also difficult to consider the possibility of a process in which they are condensed and the reason for the low pH. In some cases it may be necessary to consider the solution of sulphide from rocks or soil. In any case, the geothermal fluid that characterizes this region is vapor including a noncondensable gas which mainly consists of CO₂ and hot spring water in the shallow section that characterized by NH₄-HCO₃. Others include Lag. del Volcan on the east of the summit of VN. Copahue, where it may be possible that the volcanic gas mainly consisting of HCl and SO₂ (or H₂S) has been blown. It may be that soluble materials, such as Cl, SO₄, etc. are contained in this lake water which affect the river water downstream. The composition of fumarolic gas at Chancho Có is slightly closer to that of volcanic gas than that of Las Máquinas, Las Maquinitas, Anfiteatro, and Termas de Copahue, suggesting a correlation with the VN. Copahue.

While the origin of hot spring water is almost certain to be the meteoric water which fell in the periphery in the relatively recent past, more possibility that the geothermal fluid in the reservoir is a mixture of meteoric water and volcanic gas is pointed out, and although the relation between CO₂ gas and volcanic gas may be considered, it merely remains an assumption. According to D'Amore et al. (1987), from the ratio of N₂, Ar and He in the gas, the participation of magmatic gas is indicated for COP-1 and -2

Whether or not a hot water system exists deeper than this reservoir can be estimated from the origin of the vapor-dominated system, no geochemical evidence to support its existence in this area has been obtained.

It is considered important to monitor the change in gas vapor ratio and gas composition of COP-1 and COP-3. Especially, it is necessary to grasp accurately the density of H₂S.

5.1.5 Well Investigation

1. Thermal Gradient Holes

(1) Geology

In this area, 17 holes with a depth between 11 and 200 m were drilled by Yacimientos Petroliferos Fiscales (YPF) between 1974 and 1976⁽²⁸⁾. Data on the geology and the results of hole temperature measurement of 14 holes were collected this time.

Fig. 5-22 shows the geologic correlation including COP-1, -2 and -3. The upper 10 m of most of these holes were found to consist of the basaltic andesite in the Las Mellizas Formation. In the six holes drilled on the east side of the caldera basin, lake sediments such as conglomerate, sandstone, and mudstone were observed beneath the andesite by YPF. Of these, the mudstone of the PC-1 core between 117 and 120 m was able to be observed in the YPF laboratory.

(2) Temperature Distribution

In order to grasp the features of temperature distribution in the surveyed area, the temperature vs. depth diagram of the thermal gradient holes (Fig. 5-23) was prepared based on the temperature logging data⁽²⁸⁾ obtained from each hole for use as basic data for predicting underground temperature. Several temperature logging for each hole were performed during 2-3 months.

Based on the results of the hole temperature including COP-1 and -2, and the distribution of hot springs and fumaroles, a map of isotherms at 50 m depth was prepared (Fig. 5-24).

- (a) The high temperature zone of above 25°C is shaped like a triangle surrounding the area containing evidence of geothermal activity and corresponds to the upheaval zone with a high resistivity basement as detected by electrical prospecting. This high

temperature zone encompasses hot spring and fumarole zones which are distributed along the fissures.

- (b) In the areas to the east and southwest of this high temperature zone the temperature drops abruptly. To the north, the temperature is assumed to also drop abruptly, though it is not certain as there is no hole.
- (c) Toward the direction of Lago Agrio, an extension of the isothermal line of 15°C is seen. The hole temperature of the thermal gradient hole in the vicinity of the north side of Lago Agrio shows that it is the deep rise type, suggesting a high temperature in the deep zone.
- (d) Fumaroles are seen in the Chancho C6 alteration zone, making PC-9 near the Chilean border high in temperature. Because a fault running in the WNW-ESE direction from Chancho C6 is recognized, it is assumed that the high temperature zone extends from Anfiteatro through Chancho C6.
- (e) The map of isotherms at 50 m depth mentioned above is in concordance with the map of heat flow distribution (EPEN data)⁽²⁹⁾, indicating the thermal structure of the shallow section.

2. Exploratory Well COP-1

This well is located 2005 m above sea level on the south shore of Lag. Las Mellizas (2). It was drilled between February 1976 and March 1981, during which drilling was suspended once at a depth of 954 m and resumed in 1981. Drilling stopped at 1414 m due to accidental losses of strings. The final hole diameter was 8-1/2 inches and a production casing of 9-5/8 inches and a perforated pipe of 7 inches were inserted to a depth of 736 m and 1132.29 m, respectively, with the deeper section being assumed to have been buried. Production tests have been performed intermittently since April 5, 1981.

(1) Geology

Cuttings between 20 and 948 m and spot cores (458 - 463 m, 630 - 631 m, 930 m) were sampled from this well and we were able to observe them at the YPF laboratory this time. As shown in the integrated columnar section of COP-1 (Fig. 5-25), the geology of this well consists of the Las Mellizas Formation between the ground surface and 948 m, which is composed of basalt andesite to andesite lava and pyroclastic rocks. Cuttings between 60 and 80 m contains a fragments of mudstone which are correlated with the upper part of the Caviahue Conglomerate Member.

The drilling length per one bit was about 50 m from the start through 989 m, while it was about 150 m between 989 and 1414 m. This suggests that the rock was extremely easy to drill below the depth of 989 m. The geology of this section is assumed to be lake sediment from the geology of the peripheral area including that of COP-2, which will be described later. According to the CREGEN data, it is assumed that the drilling had re-entered the lava and encountered the lost circulation zone because the hardness of rocks increased near the bottom of the hole.

(2) Alteration

Using 9 specimens (130 - 930 m) provided by YPF this time, X-ray analysis was performed this time (Table 5-10). The results thereof suggest a division into three zones, as follows:

The zone shallower than 458 m is characterized by montmorillonite. The zone between 458 m and 930 m is composed of quartz + chlorite/ montmorillonite mixed layer-mineral which contains montmorillonite, chlorite and laumontite. The zone between 801 m and 930 m is characterized by quartz + chlorite which contains prehnite, and epidote can be seen with the naked eye.

Although the formation temperature that can be assumed from the altered minerals of this well is slightly lower than the well temperature, the specimen from a depth of 930 m immediately above the lost circulation

zone (altered andesite) was subjected to considerable alteration. Secondary minerals which are formed under high temperature, such as prehnite, epidote, and wairakite (not clear) were also detected. From this, it appears that the well encountered an active geothermal zone in the deep section, which corresponds to the temperature curve to be described later.

(3) Lost Circulation

Although detailed records on lost circulation are not available, there occurred a complete lost circulation at the depths of 830 m and 950 m. Consequently, blind drilling was adopted below a depth of 950 m. In addition, a large-scale lost circulation was recorded at the bottom, but it is probably buried at present. Therefore, the main feed zone is considered to be at a depth of 950 m. However, it is also possible that the permeability of this zone may change lower due to the lost circulation treatment.

(4) Results of Logging

When the increment drilling down to 1,414 m had been completed in the well, a series of temperature loggings were performed during the water injection, after the water injection, and after the production test in the early stage, from which the position of the main permeable zone is assumed to be near 940 m, 1060 m and 1410 m. Considering jointly with the records of lost circulation during drilling, the main feed zone that contributes to the steam production of COP-1 is assumed to be near 950 m.

The temperature that is considered the closest to the formation temperature is shown in the temperature vs. depth diagram (Fig. 5-26). Although the maximum temperature is not clear as it exceeded the measurement range of the Amerada gauge, it is convincing that it would be between 1200 m and 1370 m and higher than 250°C.

Fig. 5-27 shows a recapitulation of the representative profiles of temperature and pressure in the dynamic and static conditions of this well.

Looking at the pressure profile under the static condition, it shows a practically constant pressure gradient for the vapor phase from the well head to the bottom of the hole. In the wellbore, no pressure gradient showing the liquid phase could be seen, suggesting that the vapor and water are in a saturated condition under the reservoir condition. Considering the average of actually measured values, it can be assumed that the reservoir fluid pressure is about 35 - 38 ata and the temperature about 240 - 246°C, suggesting a saturated condition.

The results of electrical logging (induction logging) are shown in the integrated columnar section (Fig. 5-25). When the geology is compared with the results of this logging, it generally accords; lava generally indicates a high resistivity value and pyroclastic rock indicates a low resistivity value of lower than 10 ohm-m.

(5) Well Test on Permeability

At this well, a injection test was performed after the drilling was completed and the pressure transient at a depth of 950 m during the water injection was measured using an Amerada gauge. According to LATINOCONSULT/ELC-Electroconsult (1981)^{c2}, the Injectivity Index (I.I) of this well was obtained from the results of injection testing, i.e. 2.3 l/sec/kg/cm² (= 8.3 m³/h/kg/cm²). With the qualifying remarks that the results of analysis cannot necessarily be accurate, because the injection rate was unstable, the following two points were mentioned:

- The transmissivity of the main feed zone is 9.4 $\frac{\text{d-m}}{\text{cp}}$.
- Due to lost mud water during drilling, the well damage can be recognized (= skin effect).

In many cases it is difficult to express a degree of permeability of the formation that truly contributes to production from the results of

the injection test. Therefore, a calculation of the productivity index (P.I.) of this well was carried out using the results of the dynamic temperature and pressure measurement carried out on April 11, 1981 (Fig. 5-27).

From the pressure differential between the static and dynamic pressure at a depth of 950 m^{c2)} -- P.I. = 0.72 m³/h/kg/cm².

From the above, it is clear that the permeability of the reservoir that is penetrated by this well is relatively low and that the productivity is not so good.

(6) Production Characteristics

Since the commencement of production testing in April 1981, it has been conducted continuously in this well except for several interruptions in-between. The well produces mostly dry steam containing 1 - 1.5 volume % water, and the steam contains 6 - 7% (molar concentration) of non-condensable gas, (mainly CO₂).

Fig. 5-28 shows the well output characteristic curve plotted using the mass flow rate and almost all data of wellhead pressure at that time. The history of the mass flow rate and wellhead pressure is shown in Fig. 5-29. CREGEN plotted the measured values of the flow rate and other estimated values which were formalized into data of the wellhead pressure of 8 ata by means of the theoretical output curve that was calculated based on the historical data and using the semi-empirical equation of Rumi (1972). CREGEN then prepared the schematic production curve as shown in Fig. 5-30.

As shown in Fig. 5-29, with regard to longterm fluctuation in continuous production testing, during the three year period from 1982 to 1987, a decline of flow rate of about 4 t/h, was observed. According to the data in 1987 which was obtained during the production test of several months after a fluid had been shut in the well for a long term, the fluctuation of flow rate during this time cannot be defined since the conditions of measurement are not known.

3. Exploratory Well COP-2

This well is located about 2120 m above sea level on the north of Lag. Las Mellizas and is 1241 m in total depth. Drilling commenced in February 1986 under the management of CREGEN and was completed in 38 days. Drilling below a depth of 736 m was performed using the air drilling method. The final hole diameter was 8 inches, a production casing of 9 5/8 inches was inserted down to 674 m, and a perforated pipe of 7 inches down to the bottom of the hole. Production tests were performed intermittently from March 30, 1986 to November 14, 1987.

(1) Geology

Cuttings were kept and we were able to observe them at CREGEN this time. As shown in the integrated columnar section of COP-2 (Fig. 5-31), the geology of this well consists of the Las Mellizas Formation between the ground surface and the bottom of the hole (1241 m), which is composed of basalt to andesite lava, pyroclastic rocks, and sedimentary rocks. Although the cuttings form fine grains because of the use of air drilling below 736 m, in the cuttings between 814 m and 1160 m lake sediments, apparently consisting mainly of tuffaceous mudstone, are distributed, and this is correlated with the lower part of the Caviahue Conglomerate Member. This member contains some intercalated lavas and pyroclastic rocks.

(2) Alteration

Although the zones that were strongly altered are fewer compared with COP-1, the rocks between 610 m and 814 m show such severe alteration that the texture of the original rocks cannot be seen and that secondary minerals, such as pyrite and epidote can be seen in quantity. Also, the rocks between 408 m and 472 m were altered, pyrites occurring.

The results of the X-ray analysis performed this time (Table 5-10) can be divided into the two zones shown below as in the case of COP-1.

The zone between 415 m and 643 m is characterized by quartz + chlorite/montmorillonite mixed-layer mineral, which contains montmorillonite and chlorite. The zone between 643 m and 1205 m is characterized by quartz + chlorite + epidote, which contains prehnite and wairakite.

The formation temperature that can be estimated from the altered minerals of this well is concordant with the well temperature and is higher than COP-1. However, the zone below the depth of 1160 m shows weak alteration and a few altered minerals formed under high temperature were observed.

(3) Lost Circulation

Although the details are not known below a depth of 736 m because of the use of air drilling, many lost circulations occurred in lava. The main production zone is considered to exist at the depths of 872 m and 1132 m from various logging data, which correspond to the lava.

(4) Results of Logging

The temperature that is considered the closest to the equilibrium formation temperature is shown in Fig. 5-26. The temperature in the section below a depth of 600 m is generally constant and the maximum temperature is 234.7°C at 950 m and 1,000 m. The lower temperature at 1,150 m is considered to be due to the effect of cold water being injected and the actual formation temperature is estimated to be about 235°C.

Fig. 5-32 shows a summary of the temperature and pressure profiles for the static and dynamic conditions of this well. Viewing the average of the measured values, it can be estimated that reservoir pressure is about 30 ata and the temperature about 235°C.

The static pressure gradient measured on April 13, 1986 down to a depth of 1150 m, indicates to be in parallel with the case of 100% gas between the depths of 100 m and 700 m, parallel with the pressure gradient of steam between the depths of 700 m and 1150 m, and it is

assumed that the non-condensable gas (mainly CO₂) concentrates on the top of the static well. Both the dynamic and the static pressure profiles show the hydrostatic gradient of water below the depth of about 1150 m, from which it is considered that no fractures exist between 1150 m and the bottom of the hole. Fig. 5-31 shows the results of electrical logging (dual laterolog). No correlation with the geology can be seen. Although the reason for this is not definite, it may be due to the effect of vapor phase.

(5) Permeability Test

A water injection test was performed by setting the Amerada gauge at the designated depth (1050 m) after the completion of drilling. When calculating the injectivity index (I.I) using the pressure data during the period of water injection for 20 minutes at each stage at the injection rates of 593, 844, 1050 and 1278 l/min., the average I.I = 7 m³/h/kg/cm² was obtained.

Although no definite statement can be made as to the productivity index, as the flow rate data when the dynamic temperature and pressure logging was performed are not known, the trial calculation of P.I. was made assuming that the flow rate at that time was about 16 t/h and using the flow pressure at a depth 1100 m, which was measured on April 12, 1986, resulted in 0.59 - 0.75 m³/h/kg/cm².

According to EPEN (1986)c30, the value of kh = 5.18 darcy-m, skin factor = 0 was reported. Although it was reported that they were calculated from the wellhead pressure, the details of the original data are not known. Fig. 5-33 shows the results of the plotted buildup data of the wellhead shutin test performed on April 8, 1986, which were obtained by the JICA Team this time. From this data, kh (permeability. thickness product) = 3.4 darcy-m, S = -1.3 were obtained, which are close to the values reported by EPEN.

Judging from the results of various well tests, well damage was not seen, but it is considered that the permeability of the reservoir

layer, that is penetrated by COP-2, is relatively small and the productivity of the well is not so large.

(6) Production Characteristics

Production tests were performed on this well from March 20, 1986 to November 14, 1987, except for a suspension of about 3 months. The well produces mostly dry steam which contains 6 - 10% (molar concentration) of non-condensable gas, mainly CO₂. Fig. 5-34 shows the well output characteristics curve plotted. The history of the mass flow rate and wellhead pressure is shown in Fig. 5-35. Fig. 5-36 shows the schematic production curve which CREGEN prepared using the semiempirical equation of Rumi (1972).

The well characteristics curve (Fig. 5-34) shows that the production data of April 1986 indicates the configuration of one curve. The measurement values of production characteristics obtained a year later in April 1987 scatter, as shown in the figure, therefore, suggesting the possibility that the data was not measured under stable conditions. If the JICA team were to draw a curve, the flow rate would be about 11 t/h and about 6 t/h at wellhead pressure at 4 ata and 13 ata, respectively, meaning a decline in the mass flow rate of some 4 - 5 t/h in a year. In November 1987, after continuous production tests for about 8 months, the mass flow rate was about 7 t/h at 6 ata.

The decline of the mass flow rate above is also shown in the production history as shown in Figs. 5-35 and 5-36.

4. Exploratory Well COP-3

(1) Selection of Drilling Site

The location of the exploratory well COP-3 was selected after a field reconnaissance and a deliberate analysis, based on geophysical and geochemical surveys and well test results between December, 1987 and

January, 1988. Reasons for the selection are described in the progress report, a summary of which is as follows:

In the Copahue geothermal area, a triangle area of 13 km² was selected as having a geothermal reservoir from the geological structure, temperature distribution, and electric resistivity distribution. Four geothermal manifestations including Termas de Copahue and exploratory wells COP-1 and -2 are also located in this area. These two exploratory wells were confirmed to have the vapor-dominated reservoir below a depth of 800 m, although their productivity is not very high.

In an attempt to find a fault zone which was expected to yield a high productivity in the triangle zone, three locations, A, B and C were chosen for the possible site of COP-3. The locations of the three sites are shown in Fig. 5-50 and 5-51, and their respective features are shown in Table 5-11. The three points constitute a regular triangle with each side measuring 2 km, which covers the central portion of the above mentioned prospective geothermal triangle. Drilling these three points was recommended to accurately evaluate the amount of reservoir.

Point A was positively chosen as the first priority from the three candidates for the following reasons:

- (a) This site is located along the WNW-ESE predominant fault. Discharging from COP-3 is expected since Chanco C6, Las Máquinas, and COP-1 are located over this fault.
- (b) Since this location and COP-1 and -2 form a triangle with a side length of 1 km, it is useful to extend areally in making a reservoir assessment in addition to the data of COP-1 and CO-2.
- (c) It provides good accessibility in the limited period for making the preparation for drilling.

(2) Drilling Operation

The existing exploratory wells COP-1 and -2 were drilled to a depth of 1,414 m and 1,241 m respectively with large diameters using a rotary drilling machine. For obtaining information at a further depth by core drilling, the target depth of COP-3 was set at 1,800 m, which is considered to be the upper part of the Hualcupen formation, the possible location where a hot water reservoir exists.

The boring machine used for drilling COP-3 and the equipment which was not available in Argentine were supplied by JICA. This boring machine has functions for both rotary and spindle drilling, with a drilling capacity of 2,000 m using NQ bits (outer diameter: 75 mm).

Drilling operation was carried out with a drilling team organized by EPEN under technical consulting by drilling engineers from JICA. The improvement of the road extending 1 km along the lake coast of Las Mellizas from COP-1 and the leveling of the boring site were completed by EPEN in December, 1988. The substructure made in Neuquén and the boring machine from Japan were assembled and drilling started on January 17, 1989.

Drilling of COP-3 was originally planned to be completed between October, 1988 and May, 1989. Because of a number of troubles encountered during drilling, the work was significantly delayed and, after discussions with JICA and AREXA, the work was continued over three periods: from October, 1988 through May, 1989, November, 1989 through March, 1990 and December, 1990 through May, 1991.

The winter of 1991 came earlier than usual and work was disrupted by the first heavy snow in April 15 when NQ-WL drilling from the 1,000 m depth started after inserting a 92 mm casing pipe down to 982 m (4 1/8-inch drilling down to 1,000 m). After discussion between JICA and AREXA, it was decided to stop drilling on April 27 for well completion and the schedule for preparation of the well test was made. In the meantime the drilling was to be continued as deep as possible. NQ-WL drilling was continued with the total lost circulation, after the lost

circulation occurred at a depth of 994.7 m occurred during drilling cement. The drilling was finished on April 27 at a depth of 1,065 m.

After drilling was stopped, electrical logging and temperature logging were conducted and a 2-inch slotted pipe was installed between the depth of 986 m and the bottom hole. Then an injection test and temperature recovery survey were conducted. The casing program is shown in Fig. 5-37.

The production test on CP-3 was commenced on June 1, 1991, installing production test facilities with a recorder system in a snowstorm. Thus well tests were carried out by the JICA team. The tests included measurement of temperature and pressure in that well before (on May 31) and during production (on June 12-15), as well as a buildup test after stopping production, etc. At the same time, the following tests were implemented on COP-3: Observation of core cuttings, X-ray diffraction, fluid inclusion measurement and core test of physical property. The results of the laboratory tests and well tests are described below.

(3) Geology, Alteration and Physical Property

(a) Geology

COP-3 drilling site is located 30 m from the east shore of Las Mellizas upper lake, 20 m from the south shore of Rio Mellizas.

The riverbed of Rio Mellizas exposes andesite lava. The surface soil is less than one meter thick at the COP-3 drilling site.

The geology of COP-3 is shown in Fig. 5-38 (Columnar section of COP-3).

The Las Mellizas formation of the early Pleistocene composed of volcanic products and lake deposits, is distributed from the wellhead to the bottom hole at a depth of 1,065 m.

The layers from the surface to a depth of 70 m are composed mainly of hyperthene basaltic lava and intercalate a thin tuff breccia. The layers from 70 to 210 m are made up largely of andesitic and dacitic altered coarse tuff and intercalate an andesite.

Between 210 and 420 m, two pyroxene basaltic andesite lavas are distributed. Altered lapilli tuff is between 300 and 320 m.

Between 420 and 480 m, tuffaceous mudstone, sandstone and conglomerate, which are considered to be lake deposits locally accumulated, are distributed.

At a depth between 480 and 830 m, pyroxene basaltic lava is distributed. These pyroxenes are all made up of augites. A tuffaceous sandstone layer is distributed between 620 and 640 m. Alteration mineral, epidote, occurs widely, filling cracks. Below 800 m, rocks are hydrothermally altered.

At a depth of 830 to 876 m, altered tuff breccia is distributed and intercalates andesite lava.

Between 876 and 1,008 m strongly altered andesite lava almost brecciated is distributed, causing frequent lost circulations by mud water during drilling.

Particularly between 1,009 and 1,018 m, andesite lava is sheared by a fault constituting a fault zone. Many lost circulations happen in this zone, which is the main production zone of COP-3.

Between 1,026 m and the bottom hole at 1,065 m is holocrystalline porphyrite, almost free of cracks.

(b) Cracks and Faults

NQ size core drilling was conducted between 782 and 882.9 m and between 1,000 and 1,065 m. Between 782 and 882.9 m, it is

considered that the following two zones are related to the fault among several no-core zones.

- 814.1 - 818.7 m
- 821.2 - 822.1 m

Cores in close vicinity to these zones are brecciated by the fracture, which is considered to be an opening fault since it coincides with the depth of lost circulation. No cores were either taken from between 785.0 and 785.4 m and between 790.6 and 792.2 m. The former was due to core plugging in a core tube during drilling and the later does not show the clear relationship with the fracture due to no coincidence of the depth of lost circulation.

Between 823.4 and 823.8 m, cores are brecciated by fracture which is considered to have some relation with the lost circulation. Between 801.7 and 802.7 m, quartz and calcite druse and the open cracks were observed, and are considered to have some relation with the lost circulation.

Between 1,000 and 1,065 m, one flow unit of andesite is distributed from the depth of shallower than 1,000 m to 1,017.5 m, and the bottom of which is brecciated. A fault extends through this point and the fracture zone is made up of three or four main and sub-main faults. In this zone, the core is fragmented into 3 ~ 5 cm, and it is considered to be a secondary path of geothermal fluid, suffering strong alteration on the nearby zone.

- 1,009.08 to 1,009.75 m: a fault which is sheared and strongly altered.
- 1,009.75 to 1,013.8 m: zone sheared in every 1 to 1.5 m interval

- 1,013.8 to 1,015.9 m: wholly fractured fault zone. Slicken side is seen.
- 1,017.3 to 1,017.5 m: small faults are observed.

Thus, the zone between 1,009 and 1,018 m is the largest lost circulation zone and also the feed zone of vapor of COP-3.

From 1,017.5 m to the bottom hole at 1,065 m, cores are massive with few cracks, most of which are filled with alteration minerals such as chlorite and epidote. Particularly, below 1,030 m, bar-like cores of three meters or more were taken out. It would permit no flow of geothermal fluid.

(c) Alteration

The degree of alteration at COP-3 changes beyond the lake deposits at a depth of 620 m in the field observation, except for comparatively strong montmorillonitization and chloritization between 70 and 210 m. The alteration is weak above 620 m on the whole with some variations of alteration. On the contrary, the alteration is strong below 620 m with chloritization. Epidote appears below 660 m, filling cracks, and epidote commonly occurs below 730 m.

Below 800 m, it is considered that three different alterations occurred, related to the geothermal fluid.

The first is the chloritization widely seen below 800 m. The lower part of Las Mellizas formation is chloritized widely and almost evenly in the graven structure.

The second is the existence of alteration minerals such as epidote, prehnite, that occur in cracks. This alteration seems to have occurred before the current geothermal convection system, and these minerals filled up almost all cracks, leading to a decrease in the permeability.

The third is the existence of wairakite crystallized on the crystal plane of the above mentioned epidote in open cracks developed in the fracture zone. The wairakite suggests a good path for vapor, which makes a good productive zone.

The X-ray diffraction of COP-3 (Fig. 5-39 and Table 5-13) allows the following classification of the alteration zone:

- Below 320 m: montmorillonite + chlorite zone
- 320 to 528 m: quartz zone
- 528 to 660 m: montmorillonite zone
- 660 to 956 m: chlorite + epidote zone
[819.8 to 956 m: chlorite + epidote (+ prehnite) zone]
- 956 to 1,065 m: chlorite + epidote + sericite
(+prehnite + wairakite) zone

The lake deposits in the quartz zone and montmorillonite zone were excluded from the classification since they were considered to be not altered insitu. It shows that the alteration materials in the parentheses do not always appear. Below a depth of 320 m, the result of X-ray analysis shows a tendency that alteration minerals formed in higher temperatures appear and that those formed in lower temperatures disappear. Montmorillonite disappears at a depth of 620 m and the temperatures at this point are estimated to be about 190°C from the fluid inclusion study as mentioned below. This corresponds well with the formation temperature of quartz + montmorillonite (100-200°C) reported by Hayashi (1973). Chlorite occurs continuously below 660 m. Chloritization as well as the above mentioned montmorillonite is observed not only along cracks but over the entire wall rock, and in a core where no cracks develop. Wairakite has a strong relation with the lost circulation zone as mentioned above and is crystallized along cracks at 956 to 1,045 m.

Kaolinite formed under acid environment was detected at 200-320 m, 400-760 m and 812-854.5 m. Since it develops in the fracture zone free of lost circulation and the temperature pattern

indicates a rapid increase of temperature in the kaolinite zone, it can be assumed that kaolinite seals cracks and that the zone functions as a cap rock. The X-ray analysis conducted at Universidad Nacional del Sur reports the existence of pyrophyllite from specimens at a depth of 1,022 to 1,045 m. However, pyrophyllite is not confirmed by the microscopic observation and X-ray analysis conducted in this study by JICA. The results of measurement of physical property of core are also shown in Table 5-14.

(d) Fluid Inclusion

The homogenization temperatures of fluid inclusion of 11 samples were measured at Universidad Nacional del Sur and those of two samples were measured at JICA (Table 5-15). The three samples from 180, 210, and 320 m were quartz crystal picked up from cuttings. The 10 samples were from quartz vein and calcite vein in the core below a depth of 528 m.

Fig. 5-40 shows the homogenization temperature of fluid inclusion at a depth of 180 to 320 m, excluding the result of cutting samples. From this the following conclusions may be made.

- The homogenization temperature of primary inclusion is lower than that of secondary inclusion. This is presumably because the temperature of fluid trapped later is lower than those trapped earlier.
- While the lowest homogenization temperature of inclusion at 528 m is as low as 162.6 °C, those below a depth of 801 m are almost constant at 240 to 250 °C.
- The homogenization temperature of fluid inclusion was compared with the static temperature logging including estimated equilibrium temperature. The current formation temperature below a depth of 900 m is a constant 240 to 250 °C and the temperature decreases rapidly toward the

shallower part. The lowest homogenization temperature is very close to the temperature of logging, although the value is a little lower.

- Some gaseous inclusions are observed in the fluid inclusions in quartz at the depths of 806 and 1,013 m.

On the other hand, the lowest homogenization temperature of fluid inclusions between 180 and 320 m indicates temperatures as high as 207 to 221 °C. These temperatures were excluded from this consideration since these three samples are cuttings including many tuff fragments, so the temperature might indicate that of the deeper part. Some inclusions having the homogenization temperatures higher than 350 °C at 180 m, may indicate higher temperatures than actual formation temperature due to necking down.

From these findings, the formation temperature of COP-3 is assumed to recover further from the temperature of static logging (ST=390h 50m) conducted prior to the production test. In other words, the temperature is nearly equal to that of COP-1 which is constant between 240 and 250 °C below 800 m and is assumed to rapidly decrease toward shallower depth. The reservoir of COP-3 is assumed to be below a depth of 800 m from its temperature patterns. While there is no description of CO₂ bearing fluid inclusion, it suggests a vapor-dominated reservoir from the existence of gaseous inclusions.

(4) Lost Circulation

No lost circulation is observed above to a depth of 795.9 m in this well and frequent lost circulation occurred in the lava bed as shown in the Columnar Section of COP-3 (Fig. 5-38). The major lost circulation zones are: 795.9-828.4 m (50-total L/C; over 300 ℓ/min), 895.0-909.55 m (130-240 ℓ/min.), 954.09 m (total L/C; over 288 ℓ/min.), 980.61 m (total L/C; over 580 ℓ/min.), 991.1 m (total L/C; over 580 ℓ/min.) and 995.0 m (total L/C; over 580 ℓ/min.). After inserting the 92 mm casing

pipes down to 986.13 m, the drilling with total lost circulation down to the bottom hole (1065.0 m) was conducted.

(5) Results of Logging

Electrical and temperature logging, temperature recovery survey, well bore temperature and pressure measurements before and during production were performed in this well.

The logging results of the longest standing time are shown in the temperature vs depth diagram (Fig. 5-26). The highest temperature was 236.9 °C at a depth of 1,000 m. The temperature rises linearly up to a depth of 900 m and stabilizes at a constant level below that depth. The equilibrium formation temperatures were estimated between 240 and 244 °C below the depth of 1,000 m. The temperature curves of COP-1, -2, and -3 in shallow depth show the almost same temperature gradient. The temperature values of COP-3, however, are generally lower in the shallow depth than the other exploratory wells, particularly COP-2, which may indicate a thicker cap rock at this site; in other words, the depth of reservoir top is at a deeper level.

The well bore temperature and pressure profiles on static and dynamic conditions are shown in Fig. 5-41. The measured values of the static temperature and pressure at 1,010 m, which is a possible feed point, are shown in Table 5-16. The vapor static pressure gradient is observed between the wellhead and \sim 1,010 m. The reservoir fluid pressure at the feed point seems to be 38.16 kg/cm² and the temperature about 240 °C. This reservoir is a vapor type as those confirmed in well COP-1 and others. It is assumed that the vapor and hot water in the fracture are in saturated condition and the saturation temperature is slightly lower than that of pure water, due to the effect of CO₂. Both the dynamic and static pressure profiles show the hydrostatic pressure gradient of water below a depth of about 1,017 m, from which it is considered that no fractures exist between this depth and the bottom hole.

The result of the electrical logging is shown in Fig. 5-38. The data obtained by the electrical logging is almost in conformity with lithology. Lava generally indicates a high resistivity and the lost circulation zone indicates disordered curves. Measurements in the interval between 998 m and 1,016 m which includes the feed zone were not made because the sonde did not run down due to the collapse of the well face.

(6) Permeability Test

An injection test was performed on this well after drilling was completed. As shown in Fig. 5-42, pressure transient at 986 m was measured during the injection using an Amerada gauge. Fig. 5-43 shows the injectivity calculated from the pressure difference between the static pressure and final pressure for each injection flow rate. The pressure data is influenced by the temperature change of the water column in the well since the pressure measuring point was located above the feed zone. The average injectivity was $I.I = 38(t/h)/(kg/cm^2)$ approximately, which is larger by one order than those of COP-1 and -2.

The results of the dynamic temperature and pressure logging (Fig. 5-41) on June 13 and June 15, 1991 which were run down to the depth of feed zone were used to calculate the productivity index (P.I) of the well.

$$P.I = G / (P_{ws} - P_{wf})$$

where G = production flow rate (5.7 and 6.9 t/h)
 P_{ws} = static pressure (kg/cm²)
 P_{wf} = Flowing pressure (kg/cm²)

The productivity Indexes were obtained $PI = 17.4 (t/h)/(kg/cm^2)$ (June 13) and $PI = 3 (t/h)/(kg/cm^2)$ (June 15). Although there is a considerable difference between the two figures, these figures are significantly larger than those of COP-1 and -2, indicating the larger permeability of the reservoir. As indicated by the pressure profiles in Fig. 5-41 the productivity seems to be controlled by the well not by

the reservoir, because this well has a small diameter hole with the final diameter of NQ (78 mm) and 92 mm CP, installed on 0 - 986.13 m.

The result of the build-up test conducted on June 15, 1991, is shown in Fig. 5-44. Although this is a small diameter well as mentioned above with a small production flow rate and therefore low pressure draws down during discharge, and the pressure measurement may not be highly accurate, kh (permeability-thickness product) of 207 darcy-m and skin factor of $S=130$ were obtained. Significant well damage is observed. Since the interval of open hole (slotted liner completion; 986.13 ~ 1,065.0 m) is supposed to be much less than the thickness of an actual reservoir, the skin effect may include the influence of partial penetration. Moreover, since the flow velocity near the well bore during discharge may be considerably high, flow may not follow the Darcy's law and therefore the skin factor may be influenced also by the non-darcy effect.

From these well tests, the well COP-3 is confirmed to have reached a reservoir with a superb permeability, despite well damage and the effect of the partial penetration. A significantly high production flow rate is estimated if a larger diameter hole is used.

(7) Production characteristics

The production test was performed between June 1 and June 15, 1991 after the completion of drilling and heat recovery. The history of the production flow rate, the well head pressure and others during the 15 days are shown in Fig. 5-45. The well produces mostly dry steam (dryness: 0.92-0.99) which contains 11% (molar concentration) of non-condensable gas, mainly CO_2 . The flow rate of hot water was relatively high at the beginning due to the effects of drilling mud, etc., and was decreased rapidly as the discharge continued.

The well characteristic curve is shown in Fig. 5-46. The maximum steam flow rate of the well is approximately 9 t/h (well head pressure 1.4 kg/cm^2G). Because of the high permeability of the reservoir as mentioned above, the well had a superb discharge characteristic in

spite of the small diameter hole. The wetness of the steam increases and the specific enthalpy drops from 644 kcal/kg to 595 kcal/kg, as the well head pressure is increased by throttling the well head valve. This is presumably caused by the heat loss from the upper part of the well having a low formation temperature and by the effect of the relative permeability due to changes in the steam saturation in the reservoir near the well bore.

The long-term performance in the production characteristic of the well will be known from the results of the long-term production test. No significant changes in the steam flow rate were observed while the hot water flow rate became negligibly small according to the data obtained by the end of August, 1991.

5.2 Integrated Analysis

5.2.1 Thermal Structure

- (1) Geothermal manifestations are distributed throughout Termas de Copahue, Las Máquinas, Las Maquinitas, Anfiteatro, and Chanco C6 in the surveyed area, and a large number of fumaroles and hot springs are present, including one, in Las Maquinitas which discharges 132°C superheated steam.
- (2) The geothermal manifestations on the Argentine side are located on the horst. Thermal gradient holes drilled on the horst indicate an abnormally high temperature gradient of 25 - 35°C/100 m and temperature increases abruptly at shallow depths. Temperature in wells COP-1, COP-2 and COP-3 also increases rapidly at the shallow depth, reaching 230°C at a depth of 800 m in COP-1 and COP-3 and at a depth of 600 m in COP-2. The temperature in these wells in deeper zones remains nearly constant, but it rises again at a depth of about 1,200 m in COP-1 more than 250°C.

On the other hand, the temperature gradient up to 50 m below the ground surface outside of the horst is only 5°C/100 m. The further the distance from the horst, the lower the temperature drops abruptly. Thus, temperature differs extremely between the horst and elsewhere, and a profile of the temperature distribution up to several hundred meters below the ground level shows higher temperatures centering around the horst. In thermal gradient hole PC-4 near Lago Agrio, the temperature gradient becomes high near the bottom of the hole; and a high temperature is expected at further depth.

- (3) The production zone of COP-1, -2 and -3 is situated deeper than 800 m, and its fluid temperature is assumed to be approximately 240°C based on the logging of temperature and pressure. The temperature calculated from the gas composition of the geothermal manifestations located on the horst is 205 - 230°C, corresponding to the fluid temperature in the holes.

- (4) As compared with the outflow gas composition of the geothermal manifestations, four manifestations on the Argentine side and COP-1, -2 and -3 contain more than 90% of CO₂ whereas H₂S content is extremely low at less than 1%. On the other hand, the manifestation at Chancho C6 on the Chilean side contains around 70% of CO₂ with ten or more percent of H₂S and H₂ respectively. Therefore, Chancho C6 may be influenced by volcanic gas more than other manifestations, implying a close relationship with VN. Copahue.
- (5) D' Amore et al. (1987) suggested, based on N₂, Ar, and He ratios in outflow gas, that the fluid from COP-2 contains more magmatic component than that from COP-1. Also from the isotopic composition of the condensed water of COP-1 and -2 the original fluid is assumed to be a mixture of meteoric water and primary magmatic water.
- (6) VN. Copahue is the newest volcano in this area, and since a lava flow unit with no obvious glacial striae exists, this lava is defined to be of Holocene age. There is a crater lake near the top of VN. Copahue which is thought to become acid due to flow-in of high temperature volcanic gas consisting of HCl, SO₂ or H₂S. Thus even today, a hot magma chamber is assumed to exist underneath VN. Copahue.
- (7) The center of eruption of VN. Copahue and the Las Mellizas formation is assumed at almost the same position, which indicates that a series of volcanic activities continued from Pleistocene to Holocene time.
- (8) Therefore, the heat source of this area is assumed to be the volcanic activities of VN. Copahue and the later period of the Las Mellizas formation. The heat of the Copahue geothermal area is thought to have been conducted from the related magma chambers which are assumed to exist underneath VN. Copahue and/or the horst.

5.2.2 Reservoir Structure

(1) Geology and Geological Structure

In the surveyed area, Tertiary and Quaternary volcanic products are accumulated. As mentioned in 5.1.2 Geology, these products are classified from the lowest as follows: the Hualcupen formation of Pliocene age, the Riscos Bayos pyroclastic flow deposits of the end of Pliocene age to the beginning of Pleistocene age, the Las Mellizas formation and the A° Trolope volcanic rocks of Pleistocene age, and the Copahue volcanic rocks of late Pleistocene to Holocene ages.

After the activity of the Hualcupen formation formed a stratovolcano, a circular basin is created by a volcanic depression during the period between the end of the Pliocene to the beginning of the Pleistocene. The circular basin is approximately 19 km NW-SE and roughly 14 km NE-SW and was filled with the Las Mellizas formation consisting of andesite, basaltic rock, agglomerate, and lake sediments.

Fig. 5-47 shows a map of the Bouguer anomaly overlapped by geologic distribution. The distribution area of the Hualcupen formation corresponds with the area of ring shaped high gravity anomaly whereas the Las Mellizas formation corresponds with the area of low gravity anomaly except for the western area. In the circular basin, the horst centering around Termas de Copahue to the west indicates the area of a high gravity anomaly while the Paso Copahue-Lago Agrio Graben indicates a low gravity anomaly. The low gravity anomaly centering around the northern part of Lago Agrio is assumed to distribute thick lake sediments a part of which is seen in the thermal gradient holes.

From the results of the two dimensional analysis of gravity prospectively, the maximum depth to the basement (the Hualcupen formation) is assumed to be approximately 2,000 m on the east of Lago Agrio, and the depth in the horst zone centering around the geothermal manifestation is assumed to be 1,600 m. The horst is assumed to have been formed by upheavals due to the impact of the two volcanic activities of the Las Mellizas formation and VN. Copahue.

(2) Faults

The following three fault systems were found in the Project Area.

- (a) The NW-SE reverse fault bordering the east end of the horst centering in the Copahue geothermal area corresponds in location to the heave of the deep low resistivity layer. This is considered to indicate the argillization of the fractured zones and the rise of geothermal fluid in the deep zone on the west of the fractured zones.
- (b) The faults in the NE-SW direction are a group of new faults formed during the volcanic activities of VN. Copahue, and acting as passageways of geothermal fluid to the Termas de Copahue, Las Maquinitas, and Anfiteatro fumaroles.
- (c) The fault running WNW-ESE has predominate extention between Paso de Copahue and Lago Agrio, and acts as the passage way for geothermal fluid to the Las Máquinas and Chanco C6 fumaroles.

The fault running WNW-ESE at the north of COP-1, is thrown more than 200 m, according to the difference of the elevation of the lake sediments in the Las Mellizas formation between COP-1 and -2. This throw was also recognized from the topography at Paso Copahue.

(3) Permeability

The lake sediments in the Las Mellizas formation have a weak consolidation, but are plastic; fractures with high permeability are therefore unlikely to occur. It is also ascertained that the permeability of the mudstone found in the lake sediments is extremely small. The lake sediments have the characteristics of an impermeable layer that regulates the movement of geothermal fluid.

The main production zones of COP-1 are situated at the depths of 830 m and 950 m. Both zones are in the andesite overlying the lake

sediments. The main production zones of COP-2 are at the depths of 872 m and 1,132 m. While the former is considered to be intercalated andesite in the lake sediments, the latter is the andesite beneath the lake sediments. The main production zones of COP-3 are several fault zones developed in an andesite between the depths of 1,009 m and 1,018 m, and wairakites, presumably occurred in vapor conduits, are distributed in open fractures. These production zones are considered to be small open fractures in the rocks.

The permeability of the production zones in COP-2 is the relatively small value of $kh = 3 - 5$ darcy-m, and that of COP-1 is assumed to be almost same. In COP-3, on the other hand, the permeability is fairly high with a value of $kh = \sim 200$ darcy-m.

The considerable declines of flow rate are observed on both wells during long term production tests, especially on COP-2. One of the reasons for such a decline is probably the relatively low permeability of the reservoir.

Changes in the isotopic compositions of COP-1 and -2 indicate that the amount of fluid in the reservoir is smaller compared with the flow rate of both wells.

(4) Cap Rock

Hydrothermal alteration of rock in COP-1 and -2 is strong for approximately 200 m at deeper than 500 - 600 m, and an argillized zone containing pyrite appears. In COP-3, kaolinites are distributed almost continuously between the depths of 200 m and 850 m. Because of the existence of this argillized zone, the reservoir is maintained being capped with this zone.

(5) Distribution of Reservoir Assumed from Electrical Prospecting

According to the result of the electrical prospecting, the upper layer including the argillized zone between 500 and 800 m shows a low resistivity value of ± 8 ohm-m, and the lower layer which indicates the

existence of the vapor-dominated reservoir shows a high resistivity value of ± 150 ohm-m.

Such resistivity structures are seen in the upheaval area of the high resistivity basement. As shown in Fig. 5-49, the upheaval area extends in the triangle of approximately 13 km^2 , and almost corresponds to the horst which is surrounded with three fault systems of different direction. As shown in Fig. 5-48, the depth of the top of the high resistivity layer which is assumed to be the vapor-dominated reservoir is generally 400 - 800 m, and as it is situated at shallow depths on the north and east sides where the manifestations are located, the depth becomes deeper on the southwest.

A deep low resistivity layer is detected under the above mentioned high resistivity layer (deeper than 1,600 m), which suggests the possibility that a hot water reservoir containing a high concentration of brine may exist below the vapor-dominated reservoir.

5.2.3 Geothermal Fluid System

- (1) Hot spring water and steam from COP-1 and -2 are assumed to originate from meteoric water based on an isotopic composition of oxygen and hydrogen. The isotopic composition of hot spring water in Termas de Copahue differs from the composition of meteoric water which originally fell at the elevation of 2,200 - 2,300 m, and its origin is the meteoric water which fell and permeated into the ground near the hot springs.
- (2) The ^3H content in the hot spring water is similar to the value obtained from the surface water (2 - 3 TU), thus indicating that the origin of the hot spring water is meteoric water which has fallen recently.
- (3) The hot springs in Las Máquinas, Las Maquinitas, and Anfiteatro show $\text{NH}_4\text{-SO}_4$ type, whereas the one in Termas de Copahue shows HCO_3 type. These hot springs have a small volume of soluble cation material, while they contain a large amount of volatile elements. Therefore, these hot

springs are assumed to have originated from shallow ground water which was heated with steam and gases from the deep ground.

- (4) In Chancho C6 situating on the north slope of VN. Copahue, gas has a composition closer to volcanic origin compared with that of other manifestations, suggesting that Chancho C6 has a relation with VN. Copahue.
- (5) While the origin of hot spring water is almost definitely meteoric water which has fallen in the vicinity relatively recently, the recharge areas of fluid sampled in COP-1, -2 and -3 are topographically considered to be VN. Copahue and Co. Chancho C6 at a high elevation. A circulation system of this fluid cannot be defined because the isotopic composition of the fluid before being separated into steam and water cannot be estimated from its fluid geochemistry. However, as shown in Fig. 5-49, the extension of the apparent low resistivity zone corresponding to the NE-SW fault may imply that the fluid runs from VN. Copahue to a deep zone of the horst.
- (6) As described in section 5.2.2 "Reservoir Structure", three fault systems such as WNW-ESE, NE-SW, and NW-SE are considered to be closely related with the geothermal fluid systems. These faults are thought to play the role of passageways for fluid and a controlling factor of lateral flow as mentioned in section 5.2.4 "Model of Geothermal Systems".
- (7) Therefore, the fluid flow in the Copahue geothermal area can be regarded as follows:

The meteoric water which percolates from VN. Copahue and Co. Chancho C6, which are considered to be the recharge areas, is heated in a deep zone and raised along the faults bordering the horst and existing in the horst. During its course, the hot water is flushed and becomes a vapor phase. A portion of the steam and gas forms fumaroles on the ground surface, flows into the shallow ground water, and outflows as hot spring water after being heated. The water filling the crater lake of Vn. Copahue is presumed to be volcanic acidic water.

5.2.4 Model of Geothermal System

The following conceptual geothermal model has been created based on the thermal structure, reservoir structure, and geothermal fluid system which are described in the above sections (Fig. 5-50 and 5-51).

- (1) The heat source of the surveyed area is the magma chamber that caused a series of volcanic activity from the Las Mellizas formation through the Copahue volcanic rocks, and the area from VN. Copahue to the horst is assumed to have a high heat conductivity.
- (2) A profile of the temperature distribution in this area shows higher temperatures centering around the horst. Temperatures of more than 230°C are indicated at a depth of 600 - 800 m. The zone deeper than that becomes a vapor-dominated reservoir, maintaining a constant temperature between 230 - 240°C. Comparison of well bore temperature of COP-1 and COP-3, both located at the edge of the horst, with that of COP-2 located closer to the center of the horst suggests that COP-2 is nearer to the heat source.
- (3) Since the contents of ^3H in the hot spring water from each geothermal manifestation are not much different from that of recent meteoric water, its retention time is short. The water is not considered to have been supplied from the deep zones based on the isotopic composition of oxygen and hydrogen, but the water is meteoric water which was fallen relatively recently and permeated into the ground and heated by mixing of steam and gas.
- (4) The recharge area of the deep fluid obtained from COP-1, -2 and -3 is assumed to be VN. Copahue and Co. Chanco C6 at a high elevation. Although the fluid circulation system cannot be estimated from the geochemical analysis of the fluid, it may be the case that the extension of the apparent low resistivity zone ($AB/2=1500\text{m}$) corresponding to the NE-SW fault zone implies a flow of fluid from VN. Copahue to the deep horst zone. The supply of water, however, is not considered to be large because of the following reasons:

- (a) This reservoir is defined as a vapor-dominated reservoir based on the geochemistry of the hot spring water and data of COP-1, -2 and -3, and also the volume of fluid discharged from the reservoir is not large.
- (b) The WNW-ESE fault bordering the southwest of the horst is assumed to be altered and argillized, limiting the lateral flow of fluid to the horst.
- (5) Two NW-SE faults bordering the east of the horst also develop alteration along the faults, which is clearly indicated in the distribution of low resistivity and suggests the fluid flow.
- (6) According to the result of COP-1, -2 and -3, the vapor-dominated reservoir is covered with an alteration zone. This zone is assumed to form a cap rock and stops dispersion of the rising steam and controls permeation of the meteoric water at the same time.
- (7) The fluid of the reservoir is sustained in the fractures in the lava of the Las Mellizas formation, but the productivity of COP-1 and COP-2 is not very high according to the production tests. The productivity index of both wells is approximately 0.7 t/h/kg/cm^2 . In COP-3, on the other hand, the productivity was fairly high with the productivity index ranging from 3 to 17 t/h/kg/cm^2 . It is indicated by D'Amore et al. (1987) that, from the changes in the isotopic composition of COP-1 and -2 during the production tests, the volume of fluid held in the reservoir may be small, compared with the flow rate of both wells (approximately 15 t/h/well).
- (8) Based on the gravity survey and the depth of the Hualcupen formation, the basement rock is assumed to be approximately 1,600 m in the horst. The Riscos Bayos pyroclastic flow deposits, considered to be an impermeable zone, are assumed to cover the Hualcupen formation. Based on observation of the cliff of the circular landform, the upper part of the Hualcupen formation beneath this impermeable zone is a lava-dominated member, forming a reservoir of high capacity along the fractures.

(9) As faults which are closely related to the reservoirs in this area, the following three fault systems are considered based on the geology, well data, and distribution of manifestations etc.

(a) The WNW-ESE fault system running from Chancho C6 through Lago Agrio

(b) The NE-SW fault system found in the geothermal manifestation areas

(c) The NW-SE reverse fault system on the east of Las Máquinas

Fault (a) is the predominant fault in this area. The discontinuity of electrical resistivity is detected corresponding to the fault. Such an electrical discontinuity, judging from experience, usually forms a high potential reservoir. Fault (b) is considered to be the latest in this area and has openings that are closely related to the geothermal manifestations. As mentioned above, fault (c) causes the upward movement of the fluid. This fault forms the Las Maquinitas alteration zone.

Fluid is expected to be reserved along these faults and in the fractured lava nearby.

The following findings which have been defined with the previous investigations suggest the possibility of the existence of the hot water reservoir beneath the confirmed vapor-dominated reservoir.

(a) Detected deep low resistivity layer by the electrical prospecting.

(b) High temperature of more than 250°C at the bottom of well COP-1.

5.3 Assessment of Geothermal Resource

5.3.1 Outline of Methodology for Assessment of Geothermal Resource

There are several methods for the assessment of geothermal resource. A numerical reservoir simulation considering the inhomogeneous structure is generally used for assessment of an area in which enough data is available. In view of the amount of data available in this area, a simulation with complex grid structure will not yield a very meaningful result. Therefore, the sustainable power plant capacity of Copahue area was assessed in two steps, as follows.

(1) 2-dimensional numerical simulation

Based on the geothermal model for the Copahue area mentioned in Section 5, a numerical modeling of natural state for 2-dimensional cross section was conducted to refine a geothermal conceptual model.

(2) Assessment of geothermal resource by volumetric method

Parameters of the reservoir will be determined according to the refined geothermal conceptual model to assess the geothermal resource and the sustainable power plant capacity using the volumetric method. The uncertainties of the reservoir parameters will be taken into account by a probabilistic approach for calculation.

Conceptual flow of the analysis is shown in Fig. 5-52.

5.3.2 Natural State Modeling

1. Numerical Simulation Methodology

The numerical simulation was performed using 2-phase reservoir simulator that handles mass (water, vapor) and heat transfer in porous media. The simulator uses the integrated finite difference (IFD) formulation.

Geothermal systems evolve over geologic time, during which the thermodynamic and hydrodynamic conditions in the system change towards a dynamic equilibrium. The rate of this change is exceedingly small compared to the changes induced during the exploitation of such a system. Therefore, for all practical purposes, undeveloped geothermal systems are considered to be in a quasisteady state. Numerical modeling of this natural (or initial) state allows verification of the conceptual, hydrogeological model and accurate reserve estimation. A successful model will match quantitatively (or at least qualitatively) a wide range of observations and, in the process, will provide insight into important system characteristics, such as formation permeability, boundary conditions for fluid and heat flow at depth, and thermodynamic state of fluids throughout the system. Even if an unambiguous or accurate quantification of these parameters cannot be achieved, it may be possible to redefine the constraints on the various parameters that are useful for refining the system model, improving reserve estimation.

In the natural state simulation of the Copahue area, the A-A' section shown in Fig. 5-51 was chosen as a representation of geothermal system in the area to perform the 2-dimensional analysis, in view of the amount and concentration of data available. The simulation grid blocks of the section are shown in Fig. 5-53. Relatively small grids (width of 1 km) were defined for the central part where the vapor reservoir was supposed to exist, and for the deep region of the Vn. Copahue where the up-flow of gas and/or water is expected. In the vertical dimension, the model extends from +1,500 m ASL to - 2,000 m ASL, and this thickness is subdivided into 6 layers, in consideration of geology and alteration. The total number of blocks is: 10 (horizontal) X 6 (vertical) = 60. The depth in the section is 2 km.

The boundary conditions of the sides of computational volume are assumed to be constant pressure and constant temperature. The boundary conditions of the bottom surface are assumed to be impermeable and thermally insulated boundary and the heat source and mass source are assigned in the bottom layer (Z=1). The heat source of the central part is assigned a heat flow value (0.5 - 0.6 W/m²) calculated from a temperature gradient (27 - 29°C/100 m) of shallow parts (for cap rock) of COP-2 and -3. A mass source of 2 kg/s is finally assumed for the deep region of the Vn. Copahue. The boundary conditions of

the upper surface were set for permeable boundary (constant prescribed pressure) and constant temperature.

Under these conditions, the permeability was modified by trial-and-error in numerous runs to make the calculated temperature and pressure distribution agree with the actual values, reasonably, to prepare finally the natural state model. In these calculation runs, the balance of permeability of the impermeable cap rock and side barrier which are a feature of a vapor dominated reservoir, the reservoir permeability and the permeability of fracture zones for surface discharges of Termas de Copahue are mainly investigated. In one calculation run, the result of simulation time of 50,000 years is assumed to be the current natural state, and these calculated values were compared with actual measurements of temperature and pressure.

2. Results of Numerical Simulation

A final model for the area has been developed with particular attention as to whether temperature and pressure conditions in the steam/water 2-phase region agree with those estimated from actual measurement, together with its extent. 29 runs were made until the final model was obtained.

Figures 5-54, 5-55, 5-56 and 5-57 show temperature distribution, pressure distribution, steam saturation distribution, and mass flux distribution respectively, finally obtained for the two-dimensional section model of the Copahue area.

The conceptual model indicates the presence of a vapor-dominated reservoir in a zone covered by an alteration zone of Las Mellizas formation that is assumed as a cap rock, and surrounded by alteration zones and faults obtained in electrical exploration and surface reconnaissance as side barriers. The results of numerical simulation strongly support these assumptions; the 2-phase zone extends in an area surrounded by alteration zones under the geothermal manifestations such as Termas de Copahue and Las Maquinitas, from which steam rises and its portions flow into a surface ground water aquifer through fractures in the cap rock. The flow rate of vapor discharged from the upper layer is estimated at 1.6 kg/sec. The model suggests the presence of

a hot water zone deeper than Z=2, which forms an extensive hydrothermal convection system with water moving in the upper 2-phase zone. A location of the boundary between the steam and hot water zones as well as the value of steam saturation are determined by the balance between mass (steam) discharge from the upper reservoir and recharge of water from the sides. Therefore, since well data in a deeper zone is not available, quantitative analysis beyond this point does not appear to be worthwhile. Fig. 5-58 shows permeability distribution assigned in the final model.

Although field data are not sufficient to depict the state of the deeper zone, this numerical simulation has clarified a part of the thermo-dynamic conditions in the vapor-dominated reservoir heated by conduction from the deep central zone of the Copahue area, which enabled us to refine the conceptual model in quantitative aspects.

5.3.3 Assessment by Volumetric Method

1. Reserve Estimation Methodology

At the exploration stage of a geothermal system, reserve assessment is based on volumetric estimation. We have used modified version of the volumetric reserve estimation method introduced by the USGS (White and Williams, 1975; Muffler and Guffanti, 1978) in this Copahue study. We have further improved this approach, to account for uncertainties in some parameters, by using a probabilistic basis.

In volumetric method, the maximum sustainable power plant capacity (E) is given by:

$$E = AhC_v(T-T_o) \cdot R/F/L \quad (5.4.3.1)$$

where

A	=	areal extent of the reservoir,
h	=	thickness of the reservoir,
C _v	=	volumetric specific heat of the reservoir,
T	=	average temperature of the reservoir,

- T_o = rejection temperature (equivalent to the average annual ambient temperature),
 R = overall recovery efficiency (the fraction of thermal energy in-place in the reservoir that is converted to electrical energy at the power plant),
 F = power plant capacity factor (the fraction of time the plant produces power on an annual basis), and
 L = power plant life.

The parameter R can be determined as follows:

$$R = \frac{W r e}{C_f (T - T_o)} \quad (5.4.3.2)$$

- where
- r = recovery factor (the fraction of thermal energy in-place that is recoverable as thermal energy),
 - C_f = specific heat of reservoir fluid,
 - W = maximum available work from the produced fluid, and
 - e = utilization factor to account for mechanical and other losses that occur in a real power cycle.

The parameter C_v in eq. (5.4.3.1) is given by:

$$C_v = \rho_r C_r (1 - \phi) + \rho_f C_f \phi \quad (5.4.3.3)$$

- where
- ρ_r = density of rock matrix,
 - C_r = specific heat of rock matrix,
 - ρ_f = density of reservoir fluid, and
 - C_f = reservoir porosity.

The parameter W in eq. (5.4.3.2) is derived from the First and Second Laws of Thermodynamics as follows:

$$dW = dq (1 - T_o/T), \text{ and} \quad (5.4.3.4)$$

$$dq = C_f dT \quad (5.4.3.5)$$

where q represents thermal energy.

Equations 5.4.3.1 through 5.4.3.5 above can be used to estimate the reserve in terms of the maximum power capacity available from a prospect.

The following parameters are estimated for the Copahue area without significant uncertainty:

- $\rho_r C_r$ = 2360 kJ/m³/°C (typical value of rock),
- T_o = 10°C (average ambient temperature),
- e = 0.6 (typical for geothermal plants of vapor dominated type)
- F = 0.85 (typical for modern geothermal plants), and
- L = 30 years (typical amortization period for a power plant).

The remaining parameters (area, thickness, porosity, average temperature, steam saturation and recovery factor) required for reserve estimation are considered to have some uncertainty. Therefore, reserves are calculated in a probabilistic way, using the Monte Carlo simulation method.

Application of any probabilistic estimation method for recoverable reserves requires; a) the estimation of probability distributions for each of the parameters; and b) a technique for repeated sampling of these distributions.

The problem of difficulty to assign a probability distribution function to each uncertain parameter in a project is resolved for all practical purposes by assuming uniform or triangular distributions for the parameters. The uniform distribution describes a variable that has equally likely values between a specified minimum and a specified maximum. In cases of considerable uncertainty, the uniform distribution offers the only practical subjective definition for a random variable; but if judgement indicates that some portion of the range is more likely, the triangular distribution gives a better representation of the parameter.

The Monte Carlo simulation technique is a sampling procedure whereby highly complex expressions involving one or more probability distributions may be evaluated easily. In essence, it consists of simulating a process, such as the development of a geothermal field, using a random sampling of the uncertain input parameters.

The basic method of Monte Carlo simulation for resource assessment is shown in Fig. 5-59 as a schematic representation.

The results of Monte Carlo simulation can be best presented by setting up interval ranges of E from the smallest to the largest values and by counting the number of computed values (and from that, the percentage of computed values) which fall within each range. Such a diagram is a graphical expression of the underlying risks in an exploration project. For example, if such a frequency distribution has a sharp mode (that is, a small standard deviation), the underlying risks are low. Conversely, if the distribution is flat (that is, the standard deviation is large), risks are high. It is desirable to present the distribution also on a cumulative frequency (or cumulative percent probability) basis. From the cumulative frequency (or probability) graph, one can read directly the probability of achieving any specified value of the power capacity.

2. Selection of Uncertain Parameters

Calculation was performed for the following two specific areas to estimate the reserve of the Copahue area.

- a) Confirmed area
Areas where reservoir is confirmed from COP-1, -2 and -3.
- b) Whole area
Areas in the triangle (Upheaval zone of high resistivity basement detected by electrical exploration) including all geothermal manifestations such as Termas de Copahue etc.

The map of the above mentioned areas is shown in Fig. 5-60. Reserves were estimated only for vapor reservoirs since the deep brine layer estimated to exist below the vapor dominated reservoir has not been confirmed.

(1) Confirmed Area

The reserve was estimated for the area where the reservoir was confirmed from COP-1, -2 and -3 in the Copahue area. The confirmed area consists of an additional band area of 1 km width in addition to the triangle surrounded by the three wells, with each side measuring 1 km. The area encompasses approximately 4 km².

An accurate estimation of a reservoir thickness is difficult because the number of wells and their depth are not sufficient. Thickness of 600 m was chosen as the minimum value since the reservoir is confirmed at a depth of 800 m to 1,400 m (+1,200 mASL to +600 ASL) in COP-1. The maximum value is estimated to be 1,200 m based on an assumption that a reservoir extends from the depth of reservoir top (+1,400 m ASL) confirmed by COP-2 to elevation + 200 m ASL (the depth is approximately 1,800 m). Thickness of 900 m from elevation + 1,300 m to the bottom of Las Mellizas formation (+400 m ASL) is estimated to be a typical and most likely value.

The reservoir temperature of COP-2, 230°C, and the maximum temperature of COP-1, 250°C are chosen for the minimum and maximum values of the average reservoir temperature respectively. A triangular probability distribution is defined using 240°C as the most likely temperature value.

Parameters ρ_f and C_f can be obtained from the steam tables, if the temperature (T) is estimated. For the average porosity, a uniform distribution is determined with the minimum of 4% and maximum of 10%, referring to a test for the physical property of the core and typical values of the geothermal field. For water saturation, the typical immobile saturation of 0.3 is used for the minimum value and 0.5 is assumed for the maximum value. A uniform distribution was applied.

The recovery factor is the most difficult parameter to estimate. We determined the recovery factor based on the figure presented by Nathenson (1975) (recovery factor is expressed as functions of temperature, porosity and water saturation) using the maximum and

minimum values of the porosity and water saturation determined above. A theoretical recovery factor can be estimated to be 5% from the minimum values of 0.04 and 0.3 of the porosity and water saturation, respectively. This value is for a reservoir with ideal permeable condition, and practically we could assume that 75% of the bulk volume of a reservoir is porous and permeable. Therefore 0.04 was chosen for the minimum value of recovery factor. On the other hand, for the maximum recovery factor, the theoretical value in ideal conditions is 20% from the maximum porosity and water saturation of 0.1 and 0.5, respectively. Likewise, 0.15 was taken assuming 75% of the bulk volume of a reservoir is permeable for an actual condition. A uniform distribution of the probability was set for the recovery factor.

Table 5-17 is a list of parameters used for the assessment of confirmed area.

(2) Whole Area

For evaluation of the whole Copahue area, a triangle area of about 13 km² (detected by electrical exploration) which included geothermal manifestations seemed to be the maximum. Actual areal extent of the reservoir, however, may be smaller than this value. A rectangular area of 11 km² surrounded by Las Máquinas, Las Maquinitas, Termas de Copahue, Anfiteatro and COP-3, with a band area of 500 m width, was chosen as the minimum value. Since the most likely value can not be determined, uniform distribution with the maximum and minimum values of 13 km² and 11 km² was defined for the areal extent of the reservoir.

For the thickness of the reservoir, 600 m, 1,200 m and 900 m are used for the minimum, maximum and most likely values respectively the same as in the parameters for the confirmed area.

The average temperature of the reservoir was given uniform probability distribution with the minimum and maximum values of 230°C and 250°C respectively.

The same principle was applied to the average porosity, water saturation as the confirmed area. The maximum value of recovery factor, therefore, is the same value (15%). The recovery factor of 0.025 was used for the minimum value, because about half of the bulk volume of a reservoir may be porous and permeable, for the area subject to assessment, while the theoretical recovery factor is 5% for the ideal condition where the whole area is permeable.

Table 5-18 shows a list of parameters used for assessment of the whole area.

3. Results of Analysis

The results of the Monte Carlo simulation calculated from parameters mentioned in the previous section will be described for the confirmed and whole areas, respectively.

(1) Confirmed Area

Fig. 5-61 shows the frequency distribution of the calculated MW capacity. The mean value of the calculated MW capacity is 35.9 MW. The values of the uncertain parameters were sampled randomly 1,000 times, and the reserves were calculated for each sampled set of parameters. Fig. 5-62 presents plots of mean of the calculated MW values as a function of the number of trials. This figure indicates that 1,000 trials were adequate to define stable statistical results.

Fig. 5-63 shows the cumulative probability distribution of MW capacity. This figure shows that the probability is about 86% that the reserves will exceed 20 MW.

Figs. 5-64 and 5-65 show the frequency distribution and cumulative probability distribution of the reserves per unit area (MW/km^2), respectively. The mean value is $9.0 MW/km^2$. Probability is about 67% that the reserves will exceed $7.0 MW/km^2$.

(2) Whole Area

Fig. 5-66 shows the frequency distribution of the calculated MW capacity. The mean value of the calculated MW capacity for the whole area is 99 MW. The values of the uncertain parameters were sampled randomly 1,000 times, and the reserves were calculated for each sampled set of parameters. Fig. 5-67 presents plots of the mean of the calculated MW values as a function of the number of trials.

Fig. 5-68 shows the cumulative probability distribution of MW capacity. This figure indicates that the probability is about 70% that the reserves will exceed 50 MW.

Figs. 5-69 and 5-70 show the frequency distribution and cumulative probability distribution for reserves per unit area (MW/km^2), respectively. The mean value is $8.3 \text{ MW}/\text{km}^2$. The cumulative probability plot shows that there is a 58% chance of more than $7.0 \text{ MW}/\text{km}^2$.

5.4 Evaluation and Determination of Power Plant Capacity

5.4.1 Assessment of Sustainable Power Plant Capacity

The volumetric method mentioned earlier is one of the methods used for calculating reserves in a geothermal field and effectively used in the earlier stage of exploration. When detailed information on the area is obtained by further exploration, a 3-dimensional fluid flow simulation using a distributed parameter model is conducted to determine an appropriate power plant capacity, forecasting the future performance.

In assessing the sustainable power plant capacity in the area, it was decided that the volumetric method is the most suitable for the assessment, based on the investigation of the content and amount of data available.

In applying the volumetric method to the area, a study was made for two distinct areas; one for the whole area where geothermal resource is expected to exist from surface manifestations, geophysical exploration, geological structure and temperature distribution, and the other for the confirmed area where thermal fluid is confirmed to exist by exploratory wells.

1. Sustainable Power Plant Capacity in Confirmed Area

The results of the volumetric assessment in the confirmed area were described in the previous section. The cumulative probability distribution of sustainable power plant capacity by the Monte Carlo simulation shows that there is a 85% chance, which is considered to be a typical threshold, of more than 21 MW, and a 90% chance of more than 18 MW. This suggests possible capacity is more than 20 MW.

There are three wells in the confirmed area: COP-1, -2 and the currently drilled COP-3. The vapor dominated reservoirs confirmed in COP-1 and -2 are not estimated to have a high permeability. But COP-3 was confirmed to have a good permeability, in other words, good productivity. Despite its small final diameter of NQ size (96 mm), COP-3 produced the maximum steam flow rate of 9.4 tons/hr. If the production well with the final diameter of 8-5/8 is

drilled on the same reservoir temperature, fluid enthalpy and high productivity index, the steam flow rate is calculated to be 50 to 60 t/h. This corresponds to a power generation capacity of 6 to 7 MW.

Therefore, it will be possible to produce 20 MW with three or four more production wells with the same productivity as that of COP-3.

2. Sustainable Power Plant Capacity of Whole Area

No detailed drilling survey has not been made for the whole area except for the main (confirmed) area, and the reservoir temperature and permeability is assigned based on mainly estimation.

The volumetric method including the Monte Carlo simulation was used at this time to calculate reserves for the vapor dominated type.

The results of the calculation revealed that the frequency distribution curve is flat and no significant peaks are observed between 30 MW and 150 MW. The central value is 90 MW. The cumulative probability distribution indicates 95 MW at 50% probability. It would be better to assume this possibility while the survey is not yet well progressed. The cumulative probability also shows a low value; 48 MW at 85% probability, and 40 MW at 90% probability. These figures are expected to increase when the frequency distribution peaks as the survey progresses further.

A capacity of 81 MW was obtained from a deterministic approach assuming a vapor dominated type with the reservoir temperature of 230°C and thickness of 600 m.

From the above, a conservative estimate would be a 80 MW level for the vapor dominated reservoir.

For the above confirmed area, the reservoir was confirmed by exploratory wells but no confirmation has been made by wells for the whole area. Surveys like CSAMT and other effective geophysical exploration are required to define the prospect clearly, and it is necessary to confirm the existence and size of the

reservoir by drilling of exploratory wells in this prospective area. It will be highly possible to have a generation capacity of 50 MW in this area, since it is relatively easy to actually obtain one half the amount of the generation capacity estimated by the volumetric method, in view of an experimental relationship between the generation capacities of geothermal power plants in operation and reserves calculated by this method.

3. Feasibility of Water Dominated Reservoir

A water dominated reservoir is expected to exist below the depth of about 1,400 m. The deterministic approach of volumetric method was used to calculate the reserve for this region.

Calculation conditions

Areal extent of reservoir:	13 km ²
Thickness of reservoir:	700 m
Average temperature:	250°C
Rejection temperature:	10°C
Recovery factor:	0.25
Plant life:	30 years
Plant load factor:	0.85
Density of rock:	2,430 kg/m ³
Specific heat of rock:	0.972 KJ/kg°C
Utilization factor:	0.3

The result of the calculation is 141.2 MW \approx 140 MW

Although we have no direct evidence for confirming the existence of this hot water reservoir, it would be worthwhile to conduct a survey by drilling exploratory wells in view of its estimated large capacity of 140 MW.

5.4.2 Determination of Sustainable Power Plant Capacity

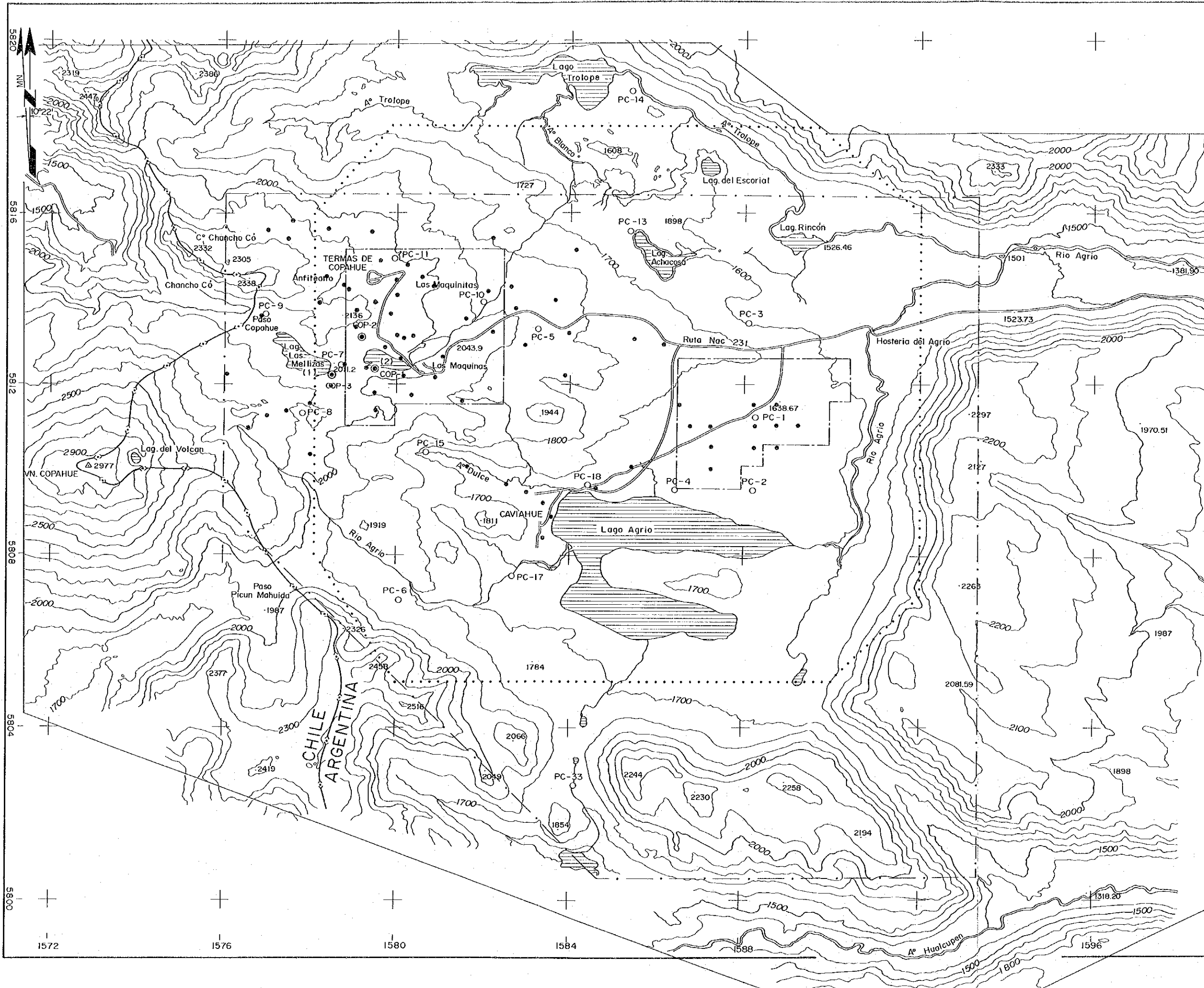
The power output of the geothermal resources occurring at a point 1,200 m deep from the surface is estimated at 10 to 50 MW with a generation period assumed

to be 30 years. Such a wide range of estimated power output means that the geothermal power development study is still at an early stage. The range tends to become narrower with the progress of the study.

At this stage, the estimated output range from 10 to 50 MW has a probability of 100 to 15%, and the output is estimated to be 20 MW with an 80% probability, and 30 MW with a 60% probability.

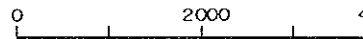
From the economical standpoint, when the unit of power station is less than 50 MW, the unit cost increases with a decreasing output, resulting in a correspondingly lower feasibility of the project. Assuming a target cost of geothermal power generation to be 0.03US\$/kWh and the probability of economic feasibility to be 90% in the case of 0.03US\$/kWh and 10% in the case of 0.05US\$/kWh, rough calculations show that the power output is estimated to be 10 MW with a 10% probability of the economic feasibility of the project, 20 MW with a 53% probability and 30 MW with an 84% probability. Thus the largest possible power output in terms of both the availability of geothermal resources and economic power generation ranges from about 25 to 30 MW. (See Fig. 5-71.)

Generally, at the early stage of a geothermal power development study the evaluated probability curve in terms of resource availability tends to incline toward low power outputs. For the purpose of the power plant design, a power output of 30 MW, a somewhat larger value, has been taken for the proposed plant capacity in consideration of such a tendency.



LEGEND

- Geological Survey
- Soil Geochemical Survey
- Fluid Geochemical Survey
- Gravity Prospecting
- Electrical Prospecting Point
- Thermal Gradient Hole
- Exploratory Well



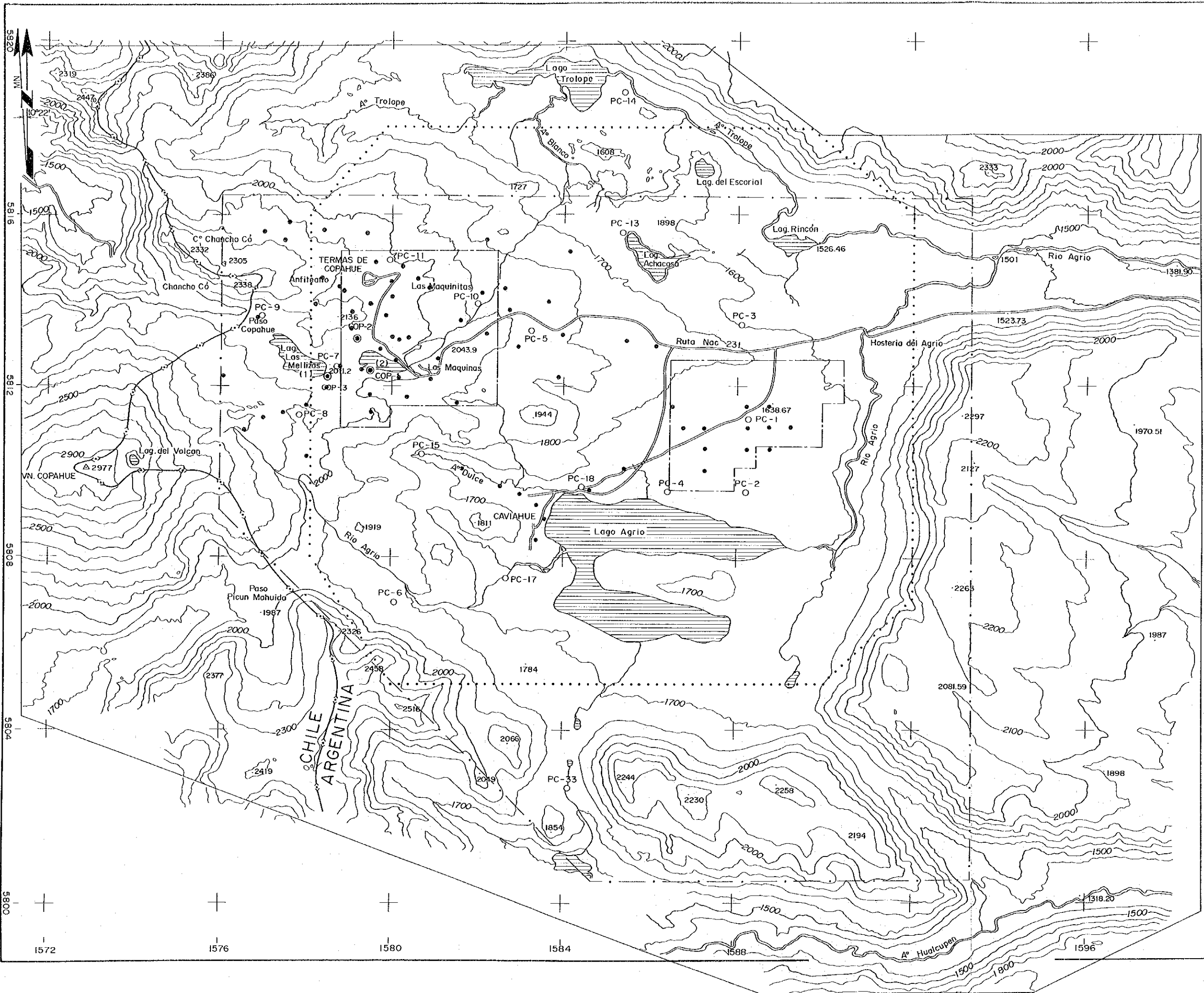
CENTRO REGIONAL DE ENERGIA GEOTERMICA
DEL NEUQUEN
REPUBLICA ARGENTINA

FEASIBILITY STUDY
OF
COPAHUE GEOTHERMAL DEVELOPMENT PROJECT

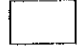
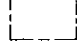





LOCATION MAP
OF
INVESTIGATION WORKS

JAPAN INTERNATIONAL COOPERATION AGENCY

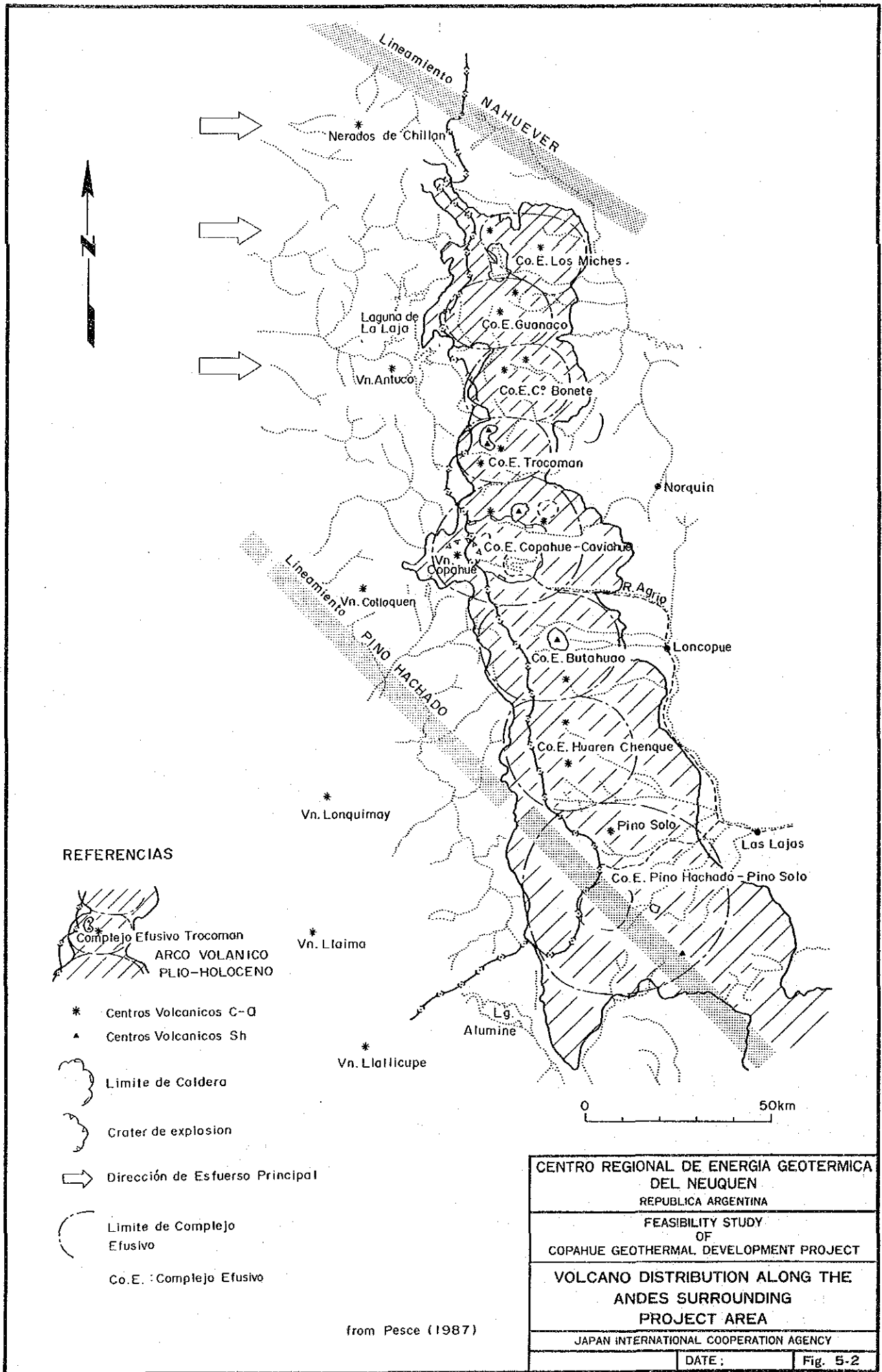
DATE: _____ FILE: _____



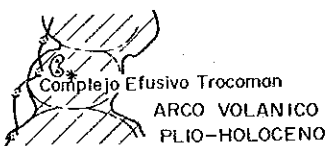
LEGEND

-  Geological Survey Photogeology
-  Soil Geochemical Survey
-  Fluid Geochemical Survey
-  Gravity Prospecting
-  Electrical Prospecting Point
-  Thermal Gradient Hole
-  Exploratory Well

CENTRO REGIONAL DE ENERGIA GEOTERMICA
 DEL NEUQUEN
 REPUBLICA ARGENTINA
 FEASIBILITY STUDY
 OF
 COPAHUE GEOTHERMAL DEVELOPMENT PROJECT
 LOCATION MAP
 OF
 INVESTIGATION WORKS
 JAPAN INTERNATIONAL COOPERATION AGENCY
 DATE: _____ Fig. 5-1



REFERENCIAS



- * Centros Volcanicos C-Q
- ▲ Centros Volcanicos Sh
- ⌋ Limite de Caldera
- ⌋ Crater de explosion
- ➔ Dirección de Esfuerzo Principal
- ⌋ Limite de Complejo Efusivo
- Co.E.: Complejo Efusivo

from Pesce (1987)



CENTRO REGIONAL DE ENERGIA GEOTERMICA DEL NEUQUEN REPUBLICA ARGENTINA	
FEASIBILITY STUDY OF COPAHUE GEOTHERMAL DEVELOPMENT PROJECT	
VOLCANO DISTRIBUTION ALONG THE ANDES SURROUNDING PROJECT AREA	
JAPAN INTERNATIONAL COOPERATION AGENCY	
DATE :	Fig. 5-2

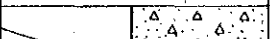
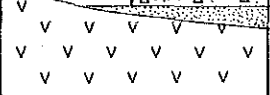

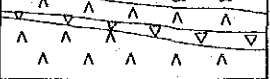
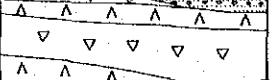

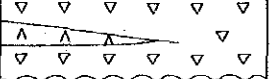

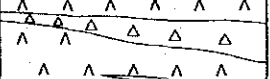
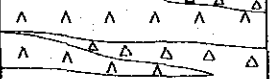
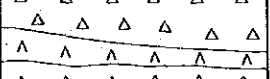
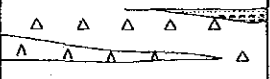
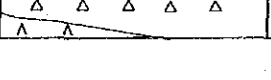
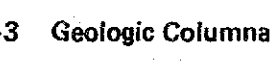


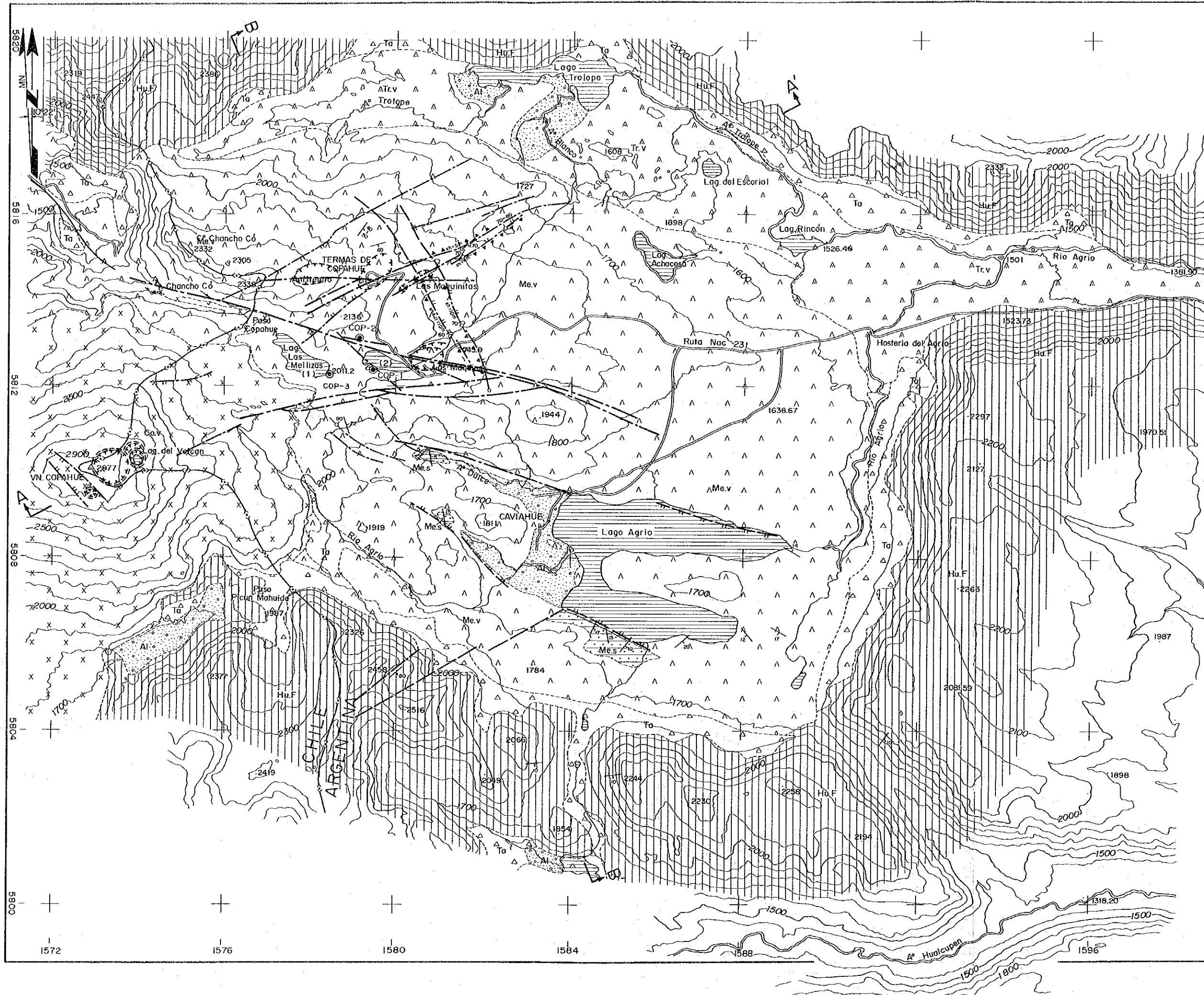
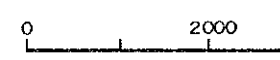
Age		Formation	Geological Column	Lithology		Remarks	
Quaternary	Holocene			Alluvium	Talus		
	Pleistocene	Copahue Volcanic Rocks		Gracial Deposits			
		A° Trolope Volcanic Rocks		Pyroxene-bearing Plagioclase Andesite			
		Las Mellizas Formation		Welded Tuff, Olivine Pyroxene Basaltic Andesite Agglomerate		Thickness • More than 1240m (in COP-2) • More than 1800m (in Chile)	
				Pyroxene Andesite, Agglomerate			
				Tuffaceous Conglomerate, Sandstone, Mudstone			
	Caviahue Conglomerate Member		Pyroxene Andesite, Agglomerate				
	Riscos Bayos Pyroclastic Flow Deposits		Biotite Pumice Tuff ~ Lapilli Tuff		Outside of the survey area		
	Tertiary	Pliocene	Hualcupen Formation		Fine Pyroxene Andesite, Olivine-bearing Pyroxene Andesite Agglomerate		Thickness More than 1800m (in Chile)
					Tuff Breccia, Tuff		
				Tuffaceous Conglomerate, Sandstone			
							
							
							
							
							

Fig. 5-3 Geologic Columnar Section of the Survey Area



LEGEND

- | | | |
|----------------------|---|--|
| Quaternary | | Alluvium
Gravel, Sand and Mud |
| | | Talus
Gravel, Sand and Mud |
| | | Copahue Volcanic Rocks
Pyroxene Olivine Basalt, Liparitic
Pyroclastic Rocks |
| Pleistocene | | A° Trollope Volcanic Rocks
Pyroxene-bearing Plagioclase |
| | | Las Mellizas Formation
Olivine Pyroxene Basaltic
Pyroxene Andesite and A
etc. |
| Tertiary
Pliocene | | Huacupen Formation
Fine Pyroxene Andesite, Agglomerate
Tuff Breccia, Tuff etc. |
| | | Geologic Boundary |
| | Strike and Dip of Strata | |
| | Fault sh: Shear Zone(m)
cl: Fault Clay(m) | |
| | Fault (Assumed) | |
| | Strike and Dip of Normal Fault | |
| | Strike and Dip of Reverse Fault | |
| | Fumaroles and Hydrothermal
Alteration Zone | |
| | Crater | |
| | Location of Section | |
| | Exploratory Well | |

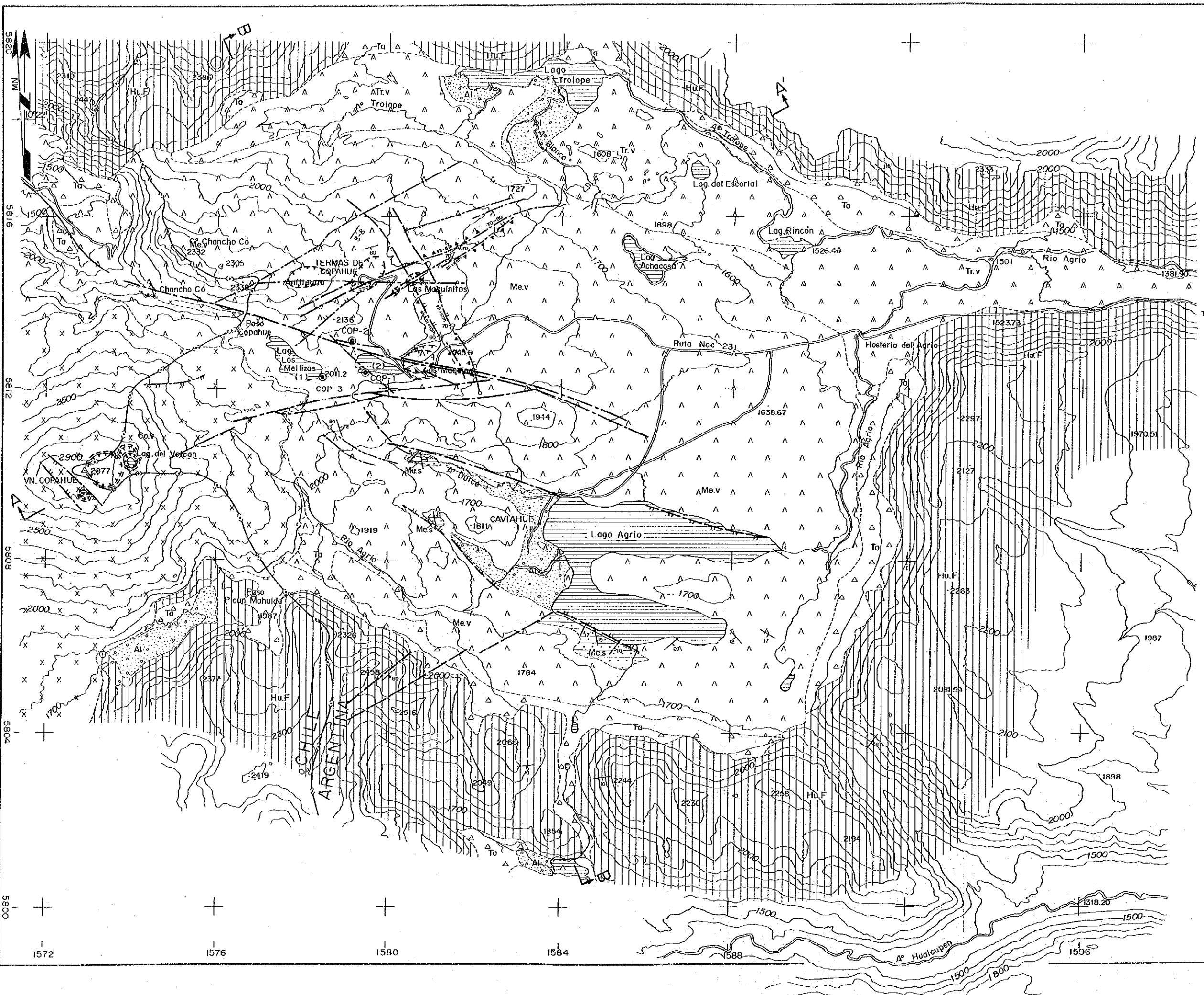


CENTRO REGIONAL DE ENERGIA GEO
DEL NEUQUEN
REPUBLICA ARGENTINA
FEASIBILITY STUDY
OF
COPAHUE GEOTHERMAL DEVELOPMENT P

**GEOLOGIC MAP
OF THE SURVEY AREA**

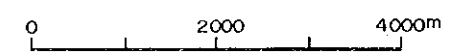
JAPAN INTERNATIONAL COOPERATION AGE

DATE: _____



LEGEND

- | | | |
|----------------------|----------|--|
| Quaternary | [Symbol] | Alluvium
Gravel, Sand and Mud |
| | [Symbol] | Talus
Gravel, Sand and Mud |
| Pleistocene | [Symbol] | Copahue Volcanic Rocks
Pyroxene Olivine Basalt, Liparite and
Pyroclastic Rocks |
| | [Symbol] | A ⁰ Trolope Volcanic Rocks
Pyroxene-bearing Plagioclase Andesite |
| Tertiary
Pliocene | [Symbol] | Olivine Pyroxene Basaltic Andesite,
Pyroxene Andesite and Agglomerate
etc. |
| | [Symbol] | Lake Sediments and Glacial Deposits
Conglomerate, Sandstone and
Mudstone |
| | [Symbol] | Hualcupen Formation
Fine Pyroxene Andesite, Agglomerate,
Tuff Breccia, Tuff etc. |
| | [Symbol] | Geologic Boundary |
| | [Symbol] | Strike and Dip of Strata |
| | [Symbol] | Fault sh: Shear Zone(m)
cl: Fault Clay(m) |
| | [Symbol] | Fault (Assumed) |
| | [Symbol] | Strike and Dip of Normal Fault |
| | [Symbol] | Strike and Dip of Reverse Fault |
| | [Symbol] | Fumaroles and Hydrothermal
Alteration Zone |
| | [Symbol] | Crater |
| | [Symbol] | Location of Section |
| | [Symbol] | Exploratory Well |



**CENTRO REGIONAL DE ENERGIA GEOTERMICA
 DEL NEUQUEN**
 REPUBLICA ARGENTINA
 FEASIBILITY STUDY
 OF
 COPAHUE GEOTHERMAL DEVELOPMENT PROJECT
**GEOLOGIC MAP
 OF THE SURVEY AREA**
 JAPAN INTERNATIONAL COOPERATION AGENCY
 DATE: _____ Fig. 5-4

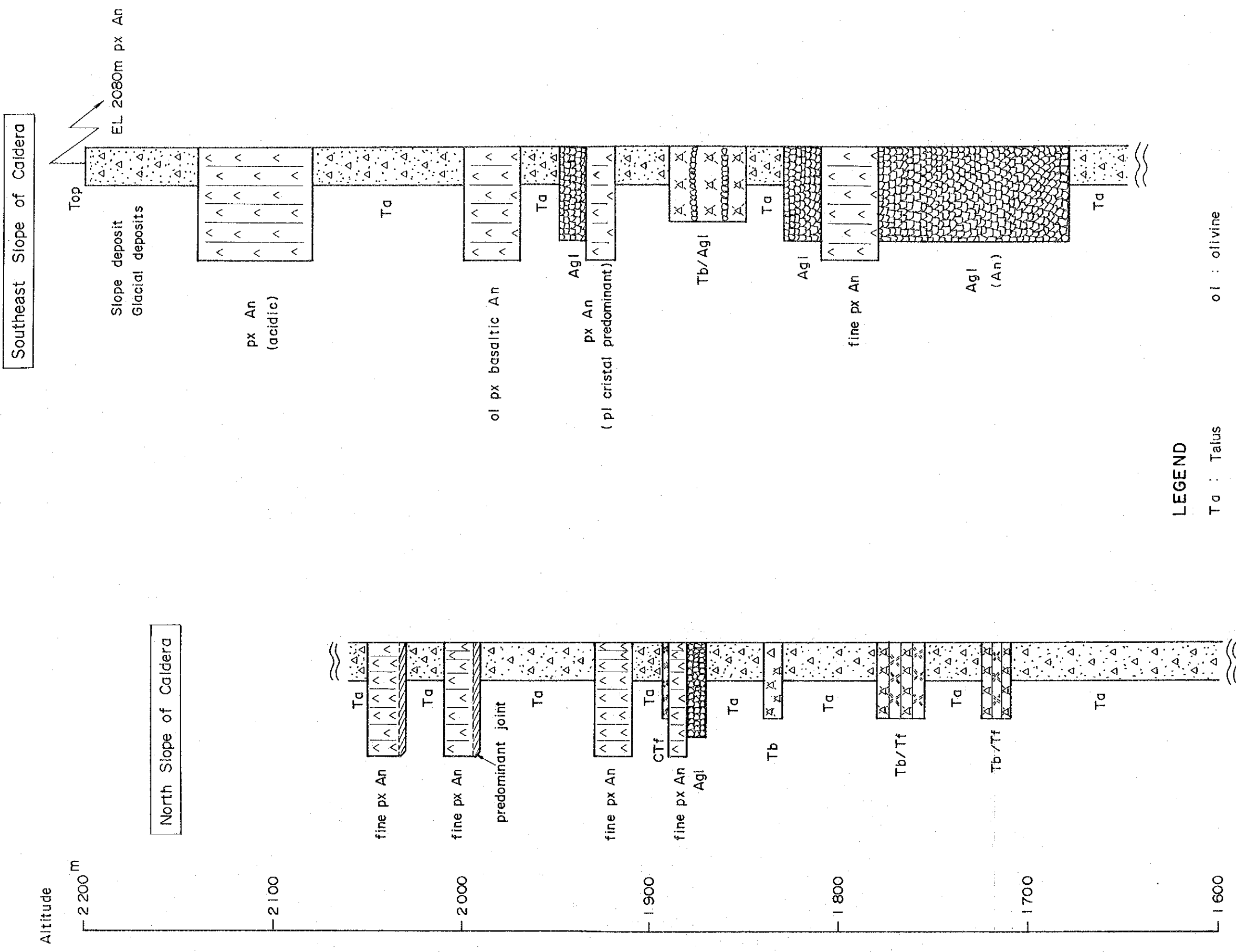


Fig. 5-5 Geologic Columnar Section of Caldera Wall